Stepwise recombination suppression around the mating-type locus in the fungus *Schizothecium tetrasporum* (Ascomycota, Sordariales)

Nina Vittorelli [1,2,3], Alodie Snirc [1], Emilie Levert [1,2], Valérie Gautier [2], Christophe Lalanne [2], Elsa De Filippo [1,2], Ricardo C. Rodríguez de la Vega [1], Pierre Gladieux [4], Sonia Guillou [4], Yu Zhang [5], Sravanthi Tejomurthula [5], Igor Grigoriev [5], Robert Debuchy [6], Philippe Silar [2]*, Tatiana Giraud [1]*, Fanny E. Hartmann [1]*

[1] Ecologie Systematique et Evolution, CNRS, Université Paris-Saclay, AgroParisTech, 91198 Gif-sur-Yvette, France

[2] Laboratoire Interdisciplinaire des Energies de Demain, Université Paris Cité, Paris, France

[3] Département de Biologie, École Normale Supérieure, PSL Université Paris, Paris, France

[4] PHIM Plant Health Institute, Univ Montpellier, INRAE, CIRAD, Institut Agro, IRD, Montpellier, France

[5] Joint Genome Institute, Lawrence Berkeley National Laboratory, University of California Berkeley

[6] Université Paris-Saclay, CEA, CNRS, Institute for Integrative Biology of the Cell (I2BC), 91198 Gif-sur-Yvette, France.

Running title: Recombination suppression around a mating-type locus

Corresponding author: Fanny E. Hartmann

E-mail: fanny.hartmann@universite-paris-saclay.fr

*co-senior authors

Keywords: fungi, *Neurospora tetrasperma,* sex chromosomes, pseudo-homothallism, evolutionary strata, mating system, interference, Sordariales*, Podospora tetraspora*

ABSTRACT

Recombination is often suppressed at sex-determining loci in plants and animals, and at self-incompatibility or mating-type loci in plants and fungi. In fungal ascomycetes, recombination suppression around the mating-type locus is associated with pseudo-homothallism, *i.e.,* the production of self-fertile dikaryotic sexual spores carrying the two opposite mating types. This has been well studied in two species complexes from different families of Sordariales: *Podospora anserina* and *Neurospora tetrasperma.* However, it is unclear whether this intriguing convergent association holds in other species. We show here that *Schizothecium tetrasporum,* a fungus from a third family in the order Sordariales, also produces mostly self-fertile dikaryotic spores carrying the two opposite mating types. This was due to a high frequency of second meiotic division segregation at the mating-type locus, indicating the occurrence of a single and systematic crossing-over event between the mating-type locus and the centromere, as in *P. anserina*. The mating-type locus has the typical Sordariales organization, plus a *MAT1-1-1* pseudogene in the *MAT1-2* haplotype. High-quality genome assemblies of opposite mating types and segregation analyses revealed a suppression of recombination in a region of 1.3 Mb around the mating-type locus. We detected three evolutionary strata, displaying a stepwise extension of recombination suppression, but no rearrangement or transposable element accumulation in the non-recombining region. Our findings indicate a convergent evolution of self-fertile dikaryotic sexual spores across multiple ascomycete fungi. The particular pattern of meiotic segregation at the mating-type locus was associated with recombination suppression around this locus, that had extended stepwise. This association is consistent with a recently proposed mechanism of deleterious allele sheltering through recombination suppression around a permanently heterozygous locus.

AUTHOR SUMMARY

Recombination allows faster adaptation and the purging of deleterious mutation but is often paradoxically lacking in sex chromosomes. It has been recently recognized that recombination can also be suppressed on fungal mating-type chromosomes, but the evolutionary explanation and the proximal mechanism of this phenomenon remain unclear. By studying here the sexual biology of a poorly studied mold living in rabbit dung, we reveal a striking convergence in three distant fungal lineages of an independently evolved association between the production of self-fertile sexual spores (carrying two nuclei with opposite mating types), a particular segregation of the mating-type locus and the lack of recombination on mating-type chromosomes, having evolved stepwise. Such a convergent association suggests causal relationships and will contribute to unveil the evolutionary causes of recombination suppression.

Graphical summary

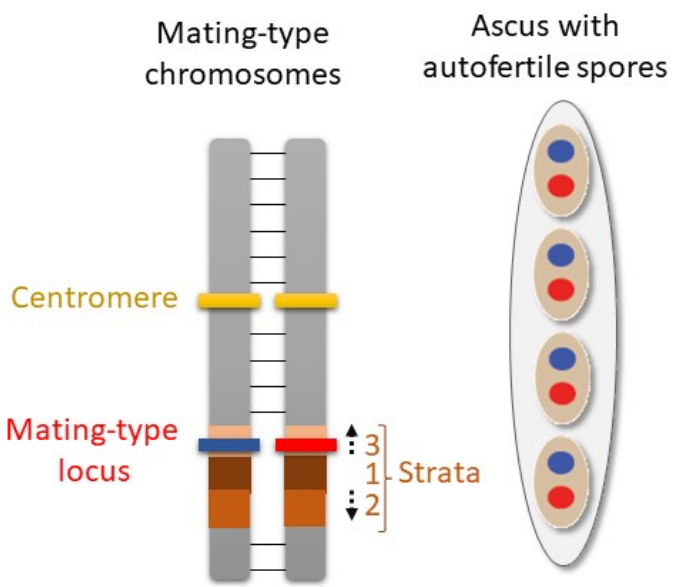

INTRODUCTION

In eukaryotes, recombination is often considered to be a major long-term evolutionary advantage. Indeed, it prevents the accumulation of deleterious mutations (1) and facilitates the combination of multiple advantageous alleles in the same genome (2). However, convergent recombination suppression events have been observed at sex-determining loci in plants and animals, and at self-incompatibility or mating-type loci in plants and fungi (3). It has been suggested that this recombination suppression links lock-and-key genes together, enabling self-incompatibility systems to function correctly (4–6). Surprisingly, recombination suppression has often been found to extend distally, in a stepwise manner, from sex and mating-type loci, generating evolutionary strata of differentiation between haplotypes (7–10). The evolutionary causes of this stepwise recombination suppression beyond mating-compatibility loci remain a matter of debate (9–12). Sexual antagonism was long thought to be the main driving force generating evolutionary strata on sex chromosomes, through selection for the linkage to the sex-determining locus of genes with alleles beneficial in only one sex (12). However, it has been difficult to obtain definitive evidence supporting this hypothesis, and evolutionary strata have also been reported in fungi without sexual antagonism or other types of antagonism between mating types (8–10,13). Alternative hypotheses have been developed (10,11), based on associative overdominance associated with the sheltering of deleterious mutations (14), dosage compensation (15) or the spread of transposable elements (16).

Fungi are useful models for studies of the evolution of recombination suppression: they have many assets for evolutionary genomics studies (17) and several convergent recombination suppression events around mating-type loci have been observed in this group (8,10,18). Fungi have highly diverse modes of reproduction, mating systems (selfing versus outcrossing) and breeding systems (mating compatibility), with considerable differences sometimes reported between closely related species (19). Among all breeding systems, heterothallism was the most investigated and seems to display the most conserved scheme in fungi (20). In heterothallic fungi, mating can occur only between haploid cells carrying different alleles at the mating-type locus. The term “heterothallism” was initially coined after observations of *in vitro* crosses, in which mating could occur only between different thalli (*i.e.,* mycelia or hyphal networks), each arising from a single spore. We now know that this heterothallism was due to the thalli mostly being haploid and carrying different alleles at the

99 mating-type locus. Other fungi were described as “homothallic” because mating within a single thallus
100 was possible. We now know that homothallism is possible because mating in these fungi does not
101 need to occur between cells of different mating types. However, some fungi capable of displaying
102 mating within a single thallus *in vitro* were later found to carry two types of nuclei, of different mating
103 types, in each cell. They were therefore called pseudo-homothallic.

104 The pseudo-homothallic breeding system has been studied in detail in two species from
105 different families of the order Sordariales (Ascomycota): *Neurospora tetrasperma* (Sordariaceae*),*
106 which is typically found as orange blooms on scorched vegetation at burnt sites after a fire, and
107 *Podospora anserina* (Podosporaceae), which is mostly found in herbivore dung. Sexual spore
108 formation is similar in these two species (21). Karyogamy occurs between two haploid nuclei of
109 different mating types, followed by meiosis, and then the post-meiotic mitosis of each meiosis product.
110 The ascus produced therefore contains eight haploid nuclei, which are packaged in pairs to form four
111 sexual spores (ascospores). The resulting ascospores are, thus, dikaryotic, *i.e.*, each contains two
112 haploid nuclei. A small fraction of asci (0.1% for *N. tetrasperma* and 1.0% in *P. anserina*) contains five
113 ascospores, with one dikaryotic spore replaced by a pair of monokaryotic ascospores (*i.e.,*
114 ascospores carrying a single haploid nucleus), recognizable in *P. anserina* by their smaller size. In
115 both species, the dikaryotic spores almost always contain nuclei of opposite mating types, and are
116 therefore referred to as heterokaryotic ascospores, each of which germinates into a self-fertile
117 mycelium (21). The particular pattern of segregation of the mating-type locus leads to the generation
118 of nuclei of different mating types in close physical proximity, which can be compacted into a single
119 ascospore. In *N. tetrasperma*, the mating-type locus segregates during the first meiotic division, due
120 to the linkage between the centromere and the mating-type locus. During meiosis II, the spindles are
121 parallel, and, following the post-meiotic mitosis, each ascospore is delineated around two non-sister
122 nuclei, resulting in the compaction of opposite mating types in the same cell. In *P. anserina*, the
123 mating-type locus segregates during the second meiotic division, due to the occurrence of a single
124 and systematic crossing-over (CO) event between the centromere and the mating-type locus. During
125 meiosis II, the spindles are aligned, leading to the same final nuclear distribution as in *N. tetrasperma*.
126 After the post-meiotic mitosis, the ascospores formed contain nuclei of opposite mating types.

127 In these two pseudo-homothallic species, there are large non-recombining regions around the
128 mating-type locus. In *N. tetrasperma*, the 7 Mb region without recombination encompasses the

129 mating-type locus and the centromere (22). In *P. anserina*, a 0.8 Mb region devoid of recombination
130 has been identified around the mating-type locus in the reference strain (23). Each of these two
131 species belongs to a complex of cryptic species (22,24,25), which also all harbor a region of
132 recombination suppression around their mating-type locus; however the size of the non-recombining
133 region differs between species within each species complex (22,26,27). In both *N. tetrasperma* and *P.*
134 *pseudocomata* (a cryptic species from the *P. anserina* species complex; (24)), the suppression of
135 recombination has extended stepwise, generating evolutionary strata (10,22,26,27). It is intriguing that
136 the presence of non-recombining regions around fungal mating-type loci and their stepwise extension
137 seem to be associated with pseudo-homothallism in ascomycetes (10). One hypothesis that could
138 account for this association is that most strains are heterokaryotic at the mating-type locus for most of
139 their life cycle in pseudo-homothallic ascomycetes. This could allow recombination suppression to be
140 selected as a means of sheltering recessive deleterious alleles, by linking them to a permanently
141 heterozygous locus (14). Indeed, non-recombinant haplotypes with fewer recessive deleterious
142 mutations than the population average should be selected for when rare, but if they increase in
143 frequency, they will start to occur as homozygotes, exposing their recessive load, unless they capture
144 a permanently heterozygous allele; in such cases, they continue to be selected and can rapidly reach
145 their maximal frequency, *i.e.* becoming fully associated with the heterozygous allele close to which
146 they appeared (14). The dikaryotic phase should also foster a stepwise extension of recombination
147 suppression around the mating-type locus by the same mechanism (14). However, studies of
148 additional pseudo-homothallic fungi are required, to assess the strength of the association between
149 pseudo-homothallism and stepwise recombination suppression around the mating-type locus.

150 We therefore studied *Schizothecium tetrasporum* (previously known as *Podospora tetraspora*
151 or *P. minuta var. tetraspora),* a third pseudo-homothallic species from order Sordariales (21,28).
152 *Schizothecium tetrasporum* belongs to the family Schizotheciaceae (also known as
153 Neoschizotheciaceae), while *P. anserina* belongs to the Podosporaceae and *N. tetrasperma* to the
154 Sordariaceae (29,30). The phylogenetic relationships between these three families are not well
155 established, but they probably diverged over 150 million years ago (31). For example, the
156 phylogenetic distance between *P. anserina* and *N. crassa,* a member of the Sordariaceae (like *N.*
157 *tetrasperma)*, corresponds roughly to that between humans and fishes (32). Phylogenetically,
158 *Schizothecium tetrasporum* is roughly equidistant from these two species (29). However, it displays

159 striking cytological similarities to *P. anserina*, particularly in terms of dikaryotic spore production: in the
160 FGSC7436 strain, 98% of asci were reported to produce four dikaryotic spores, with the spindles
161 aligned in the ascus during meiosis II (21). However, this previous study did not clearly investigate
162 whether the two nuclei of a dikaryotic spore contained opposite mating types and did not study the
163 mating-type locus or recombination suppression.

164 We identified media suitable for reproducible and fast growth, and media for sexual
165 reproduction in *S. tetrasporum.* We studied the dikaryotic strain CBS815.71, estimating the frequency
166 of second-division segregation of the mating-type locus at 99.5%. This indicates the existence of a
167 single and systematic CO event between the mating-type locus and the centromere. We also built
168 high-quality genome assemblies of homokaryons (*i.*e., with only one nucleus type) with opposite
169 mating types, making it possible: i) to elucidate the genetic organization of the mating-type locus, and
170 ii) to detect a 1.3 Mb region without recombination around the mating-type locus, through analysis of
171 differentiation between the mating-type chromosomes. We observed three evolutionary strata, with
172 significantly different levels of differentiation between mating-type chromosomes, suggesting a
173 stepwise extension of recombination suppression. We detected no increase in transposable element
174 content, non-synonymous substitutions or rearrangements in the non-recombining region.
175 Recombination suppression was confirmed by segregation analyses. Our findings indicate that the
176 convergent evolution of an extremely high frequency of self-fertile dikaryotic spores together with
177 recombination suppression around the mating-type locus has occurred in multiple pseudo-homothallic
178 fungal species.

179

180 **RESULTS**

181

182 ***High frequency of self-fertile spores in* Schizothecium tetrasporum**

183 The study of a single strain of *Schizothecium tetrasporum* (also known as *P. tetraspora*; Figure 1)
184 suggested that this species was pseudo-homothallic and produced self-fertile heterokaryotic
185 ascospores similarly to *P. anserina* (21,28), *i.e.,* with most asci containing four dikaryotic spores,
186 probably carrying both mating types. We studied the breeding system of *S. tetrasporum* further, by
187 testing different media and identifying those optimal for reproducible and fast growth, and those
188 optimal for sexual reproduction (see Material & Method section). Raju & Perkins found that the

189 FGSC7436 strain produced 2% five-spore asci. In this study, we found that 10% of the asci produced
190 by the CBS815.71 strain had five spores. We also observed, in rare frequencies, other kinds of asci,
191 including six-spore asci, and some with “extra-large” ascospores, probably encompassing three
192 nuclei, rather than the two usually encompassed during ascospore delimitation (Figure 1). The
193 resulting mycelium produced numerous asexual single-cell propagules, for which we were unable to
194 find appropriate conditions for germination and development. These cells probably, therefore,
195 corresponded to spermatia rather than conidia, *i.e.* they are sexual cells acting as fertilizing elements
196 and are unable to germinate, in contrast to asexual spores. *Podospora anserina* also produces
197 spermatia, which function exclusively in the fertilization of the female structures, the protoperithecia
198 (33). We generated an F1 progeny from the CBS815.71 dikaryotic strain, and isolated two
199 homokaryotic offspring of opposite mating types, referred to hereafter as CBS815.71-sp3 and
200 CBS815.71-sp6. The mating types of these strains were named according to the standard
201 nomenclature (34): *MAT1-1* for CBS815.71-sp6 and *MAT1-2* for CBS815.71-sp3.

202 We assessed the frequency of second-division segregation (SDS) at the mating-type locus
203 (Figure 2), by analyzing the progeny of a cross between CBS815.71-sp3 and CBS815.71-sp6. We
204 collected 190 four-spore asci (each ascus containing the products of a given meiosis) and isolated
205 large (dikaryotic) ascospores. Mating types were determined in the mycelium generated from
206 germinating ascospores, by PCR with two primer pairs, each specific to one mating-type allele and
207 yielding amplicons of different sizes. We initially genotyped only one ascospore per ascus, as this is
208 usually sufficient to differentiate between two extreme cases: first-division segregation at meiosis
209 (FDS) and second-division segregation (SDS). FDS yields four-spore asci containing two ascospores
210 of a single mating type and another two ascospores of the opposite mating type, whereas SDS results
211 in four ascospores, all containing both mating types (Figure 2A). We found that 87% (166/190) of the
212 thalli resulting from ascospore germination carried both mating types, indicating that they resulted
213 from SDS, and 13% (24/190) carried a single mating type, and were therefore either haploid or had
214 two nuclei of the same mating type. Indeed, thalli carrying a single mating type may result not only
215 from FDS, but also from the loss of a nucleus during growth in thalli resulting from SDS (Figure 2B).
216 We differentiated between these two situations by determining the alleles at the mating-type locus in
217 thalli resulting from the germination of the three remaining spores from the 24 four-spore asci in which
218 we found a single mating type in the first genotyped ascospore. Only one of the 24 asci analyzed

219 proved to be a true FDS ascus (*i.e.*, with two *MAT1-1* and two *MAT1-2* ascospores). The other 23 asci
220 contained at least one ascospore carrying both mating types, indicating that the homokaryotic thalli
221 growing from their other ascospores resulted from the loss of nuclei during growth after SDS in asci
222 (Figure 2B). We estimated the overall frequency of SDS for mating type at 99.5% (189/190) in the
223 CBS815.71 strain.

224 We detected a substantial number of homokaryotic thalli originating from SDS asci (23 thalli
225 from 189 germinating heterokaryotic ascospores), suggesting that the loss of nuclei corresponding to
226 one mating type in heterokaryotic thalli may occur at a non-negligible frequency in the CBS815.71
227 strain. Raju and Perkins (21) showed that the two nuclei present in developing ascospores undergo
228 mitosis, which is rapidly followed by the migration of two of the four daughter nuclei into the future
229 pedicel cell, which are presumed to abort, or at least to fail to contribute to the nuclear composition of
230 the resulting culture. It is therefore possible that homokaryotic thalli result from the migration of two
231 nuclei carrying the same mating type into the future pedicel (leaving two nuclei of the same mating
232 type in the maturing large ascospore cell), rather than the migration of two nuclei carrying opposite
233 mating types (leaving two nuclei of opposite mating types in the maturing large ascospore cell; Figure
234 2B). It is difficult to test this hypothesis, because there is no easy way to follow the migration of nuclei
235 during ascospore maturation. Alternatively, *MAT1-1/MAT1-2* heterokaryons may sometimes lose one
236 type of nucleus during vegetative growth.

237 We tested this second hypothesis, by determining mating type in several sections of
238 heterokaryotic thalli. A heterokaryon was generated by vegetative fusion (*i.e.*, by mixing identical
239 amounts of ground mycelia of the two homokaryotic strains of opposite mating types, CBS815.71-sp3
240 and CBS815-sp6). This procedure of mixed homokaryons chopped in very fine grain leads to the
241 generation of a heterokaryotic mycelium through multiple vegetative fusions (35) and nuclear
242 movements in the mycelial interconnected network of cells (36); no sexual reproduction can occur
243 under these growth conditions. The resulting heterokaryotic mycelium was grown on V8 medium and
244 incubated until the colony had reached 4 cm in diameter. It was then sliced into 70 pieces, each with a
245 volume of about 1 mm^3. PCR analyses demonstrated that only 31 of these 70 pieces carried both
246 mating types, 29 contained only *MAT1-2* and 10 contained only *MAT1-1*. In a parallel experiment on
247 another thallus of the same heterokaryon, the 70 pieces of mycelium were used to inoculate fresh M2
248 medium, and regenerating thalli were allowed to grow to a diameter of 1 cm. A randomly selected 1

249 mm^3 piece of each of these thalli was sampled at the edge of growing colonies and genotyped by
250 PCR for mating type. We found that 34 of the 70 regenerated thalli carried both mating types,
251 whereas 25 carried only *MAT1-2* and 11 carried only *MAT1-1*. These results indicate that one of the
252 two nuclei can be lost during vegetative growth, and they confirm the high rate of SDS in *S.*
253 *tetrasporum*, yielding 99.5% of asci with all four ascospores initially containing both mating types, but
254 with the occasional loss of one nucleus during vegetative growth. The *MAT1-1* mating type was
255 preferentially lost in both experimental set-ups (chi^2=9.25, p<0.005 for the first experiment and
256 chi^2=4.44, p<0.025 in the second experiment).

257 We investigated whether this loss of nuclei could be due to the relative fitness of the two
258 types of nuclei, by investigating whether the two CBS815.71 homokaryons, carrying either the *MAT1-*
259 *1* or *MAT1-2* mating type, displayed differences in growth rate or biomass production, and comparing
260 them with the *MAT1-1/MAT1-2* heterokaryon. We measured growth rates on three different media and
261 determined the dry weight obtained after growth on M2 medium for both homokaryons and the
262 heterokaryon (Table S1A). No significant differences in growth or biomass were found between the
263 homokaryons or between the homokaryons and the heterokaryon, the only significant effect being that
264 of culture medium on growth rate (ANOVA, Table S1B). The growth rate of the *MAT1-1* homokaryon,
265 corresponding to the mating type most often lost during growth, was slightly lower, although not
266 significantly so (Table S1A).

267

268 ***Reference genome assembly for* Schizothecium tetrasporum**

269 Using both Illumina and Oxford Nanopore MinION technology, we sequenced the genomes of the two
270 homokaryotic strains of opposite mating types, CBS815.71-sp3 and CBS815.71-sp6. We built a *de*
271 *novo* long read-based genome assembly for each, the first such assemblies to have been generated
272 for *S. tetrasporum*, to our knowledge. For CBS815.71-sp3, we also had an Illumina-based assembly
273 available that had been obtained before the long-read assemblies. BLAST searches and analyses of
274 Illumina read coverage against the CBS815.71-sp3 long read-based assembly suggested the
275 presence of bacterial contamination in the Nanopore data, but not in the Illumina data. We discarded
276 scaffolds with high similarity scores to bacterial genomes in BLAST analyses for further analyses. The
277 resulting long read-based genome assemblies for CBS815.71-sp3 and CBS815.71-sp6 contained 16
278 and 23 contigs and were 32.88 Mb and 32.83 Mb long, respectively. We found 96% of the 3,817

279 highly conserved orthologs in Sordariomycota from BUSCO analyses on the assemblies (Table S2).
280 In the CBS815.71-sp3 assembly, seven contigs were more than 3.5 Mb long and contained all the
281 conserved BUSCO orthologs. One contig corresponded to the mitochondrial genome and the other 8
282 contigs were less than 70 kb long, which is consistent with the expected number of chromosomes in
283 Sordariales, an order in which several species have seven chromosomes (28,37). Telomeric repeats
284 were present at both ends of contigs 1, 2, 4 and 5 in the CBS815.71-sp3 assembly, indicating that
285 these contigs represent four entirely assembled chromosomes (Figure 3A). For CBS815.71-sp3, we
286 compared the long read-based assembly obtained with the more fragmented Illumina-based assembly
287 and found high levels of similarity and synteny (Figure S1). We used the long read-based assembly of
288 CBS815.71-sp3 for further analyses. We found a high overall level of collinearity between the two
289 homokaryotic long read-based genome assemblies for CBS815.71-sp3 and CBS815.71-sp6 (Figure
290 3B). The 2305 indels between assemblies that we detected were scattered throughout the genome
291 and all were less than 10 bp long. These small indels were probably due to an artifactual enrichment
292 of low-complexity regions in homopolymers in the Nanopore data and were not considered for
293 subsequent analyses.
294 Repetitive sequences accounted for about 7% of the assemblies. In the CBS815.71-sp3
295 assembly, we identified 182 transposable element (TE) family consensus sequences: 4.2% Gypsy
296 LTRs and 6.7% other LTRs, 7% non-LTR SINEs and LINEs, 7.5% TcMar-Fot1 DNA transposons,
297 3.4% other DNA transposons and the remaining 70.5% repetitive sequences could not be annotated
298 (Figure S2A). Both genomes contained very few (<0.1 %) signatures of RIP (repeat-induced point
299 mutations), a fungal genome defense against transposable elements inducing C to T mutations in
300 repeated sequences at target dinucleotides (38,39).
301
302 ***Structure of the mating-type locus in* Schizothecium tetrasporum**
303 The mating-type locus was located at about the 5.180 Mbp position on contig 1 of the CBS815.71-sp3
304 assembly, which was considered likely to correspond to a fully assembled chromosome (Figure 3).
305 The mating-type locus of *S. tetrasporum* had the typical structure of heterothallic Sordariales (20),
306 with two highly divergent "alleles", referred to as idiomorphs, flanked by the *APN2* and *SLA2* genes
307 (Figure 3C; Figure S3, (40,41)). The *MAT1-2* idiomorph, present in CBS815.71-sp6, harbored a single
308 functional gene (*MAT1-2-1*), orthologous to the *mat+ FPR1* (*Pa_1_20590*) gene of *P. anserina* and

309 the *mat_a-1* gene of *Neurospora crassa.* The other idiomorph, *MAT1-1*, carried three genes (*MAT1-1-*
310 *1*, *MAT1-1-2* and *MAT1-1-3*), orthologous and syntenic with the three genes present in the *mat-*
311 idiomorph of *P. anserina* (*Pa_1_20593*, *_20592*, *_20591*) and the *mat_A* idiomorph of *N. crassa*
312 *(NCU01958, NCU01959, NCU01960). MAT1-1-1* contained the typical MATα_HMG domain
313 (pfam04769) and *MAT1-1-2* contained a HPG domain (pfam17043). *MAT1-1-3* and *MAT1-2-1* carried
314 a MATA_HMG domain (cd01389). The 3' end of the *MAT1-1-1* coding sequence was found to extend
315 outside the *MAT1-1* idiomorph in *S. tetrasporum*, as shown by its presence next to the *MAT1-2*
316 idiomorph. This truncated *MAT1-1-1* gene close to the *MAT1-2* idiomorph has a putative open reading
317 frame starting 68 residues downstreaming of the start codon of the typical *MAT1-1-1* gene structure
318 (Figure S3). However, this putative start codon is in a poor context for translation initiation, with a
319 pyrimidine in position -3 (40). The truncated *MAT1-1-1* gene encodes most of the MATα_HMG
320 domain, and the second conserved domain adjacent to the MATα_HMG domain (Figure S3; (42)).
321 This gene was therefore named *TαD1* (truncated MATα_HMG domain). This name does not follow
322 the standard mating-type gene nomenclature (34), as it is not included in the mating-type locus. TαD1
323 may be a pseudogene and its transcriptional status is unknown in *S. tetrasporum*. A similar truncated
324 *MAT1-1-1* gene is present and has little or no expression in *MAT1-2* strains in the Chaetomiaceae
325 (Sordariales) *Myceliophthora heterothallica*, *M. fergusii*, *M. hinnulea* and *Humicola hyalothermophila*
326 (43). It is unknown whether *TαD1* has any role in sexual reproduction.

327

328 ***A region with stepwise recombination suppression around the mating-type locus in***
329 **Schizothecium tetrasporum, *located 1 Mb from the centromere***

330 We plotted the synonymous divergence (d_S) between the two genomes of opposite mating types for
331 each gene along the contigs of the CBS815.71-sp3 assembly (Figure 4; Figure S4). Most of the d_S
332 values obtained were zero, as expected in a selfing species with a high degree of homozygosity. Only
333 around the mating-type locus did we find a cluster of genes with high d_S values (Figure 4), indicating
334 recombination suppression. The high degree of homozygosity throughout the genome indicates that
335 many selfing events occurred in the ancestors of the CBS815.71 heterokaryotic strain; only the
336 regions fully linked to the mating-type locus have remained heterozygous under selfing (27). Indeed,
337 for any gene linked to the mating-type locus, alleles associated with the alternative mating types
338 gradually accumulate different mutations over the time since recombination suppression.

339 Synonymous divergence (d_S) can, thus, be used as a proxy for the age of the linkage between a gene
340 and the mating-type locus (7).

341 The cluster of genes with high d_S values around the mating-type locus spanned a 1.47 Mb
342 region located between 4.983 Mbp and6.457 Mbp on scaffold 1 of the CBS815.71-sp3 assembly,
343 encompassing 406 genes in the CBS815.71-sp3 assembly and 413 genes in the CBS815.71-sp6
344 assembly. The d_S values were lowest in the center of the non-recombining region (Figure 4),
345 suggesting the occurrence of gene conversion. We found no predicted function potentially directly
346 related to mating compatibility for any of the 406 genes in the non-recombining region of the
347 CBS815.71-sp3 assembly other than the mating-type locus. A total of 15 genes in the non-
348 recombining region encoded proteins that were identified as putative transcription factors or involved
349 in signaling pathways (Table S3). The four orthologs of the *P. anserina* genes located in its non-
350 recombining region and known to be involved in post-mating sexual development (but not mating
351 compatibility) were also found in the non-recombining region in *S. tetrasporum*: *ami1*, controlling
352 nuclear migration events (44), *PaRID*, a DNA methyltransferase controlling sexual development in *P.*
353 *anserina* (45), *AS4,* encoding the eEF1A translation elongation factor and *su12,* encoding a ribosomal
354 protein, mutations of which often result in sterility in *P. anserina* (46,47).

355 The d_S values plotted along the mating-type chromosome seemed to indicate the existence of
356 three distinct evolutionary strata (Figure 4; Figure S6). We tested the existence of evolutionary strata
357 more formally, by splitting the heterozygous region with sliding limits in the CBS815.71-sp3 assembly
358 and calculating, for each limit, the difference in d_S values between the two segments; limits between
359 strata should correspond to a peak in d_S value differences according to stratum definition (27). We
360 first arbitrarily set the limit of the first stratum by eye at 5,350,000 bp and applied the automatic
361 procedure to the rest of the heterozygous region. The d_S values peaked at 5,768,335 bp, identifying
362 the limit between strata 1 and 2 (Figure S6). We then re-applied the procedure to the part of the
363 heterozygous region without stratum 2. The d_S values peaked at 5,388,708 bp, identifying the limit
364 between strata 1 and 3 (Figure S6). The median d_S values were significantly different between strata
365 1 and 2 (pairwise Wilcoxon test *p*-value = 0.00134 with the False Discovery Rate (FDR) correction)
366 and between strata 1 and 3 (pairwise Wilcoxon test *p*-value = 0.00015 with FDR correction),
367 supporting the existence of distinct evolutionary strata. Median d_S values did not differ significantly
368 between strata 2 and 3, located on opposite sides of stratum 1 (pairwise multiple-comparison

369 Wilcoxon test *p*-value = 0.27571 with FDR correction). Strata 1 and 3 each spanned 400 kb, and
370 stratum 2 spanned about 700 kb. The most ancient evolutionary stratum, stratum 1, with the highest
371 d_S values, does not encompass the mating-type locus. The mating-type locus was located in the
372 middle of stratum 3 (Figure S6).

373 We looked for the centromere on the mating-type chromosome because its position may
374 provide important insight into the segregation of the mating-type locus at the first meiotic division. We
375 found a single location with a drop in GC content along the mating-type chromosome of the
376 CBS815.71-sp3 assembly outside of the telomeric regions, with 53.5% GC between 3.990 Mbp and
377 4.025 Mbp, versus the genome-wide mean value of 58.76% (Figure S5). A drop in GC content can
378 pinpoint the centromere in some fungi, such as some *Neurospora spp.* in which GC content drops to
379 about 44%, whereas the genome-wide mean value is about 53% (48). The lower variation of GC
380 content observed in the CBS815.71-sp3 genome assembly may be due to a lack of RIP in *S.*
381 *tetrasporum*. For the other three fully assembled chromosomes of the CBS815.71-sp3 genome,
382 similar drops in GC content were also identified at a single location per chromosome, co-localizing
383 with clusters of repeats. We characterized the repeat content of these four putative centromere
384 regions. We found no specific repeats, but we did detect an enrichment in *TcMar-Fot1* DNA
385 transposons relative to the genome-wide mean (Figure S2A). The putative centromere of the mating-
386 type chromosome was located about 1 Mb from the edge of the non-recombining region around the
387 mating-type locus.

388 We found no enrichment in repetitive sequences in the non-recombining region around the
389 mating-type locus relative to autosomes and the recombining regions on the mating-type chromosome
390 in the CBS815.71-sp3 assembly. The mean repetitive sequence densities calculated in 10 kb
391 windows overlapping by 1 kb were 2.52%, 5.05% and 4.21% in the non-recombining region around
392 the mating-type locus, the autosomes and the recombining regions on the mating-type chromosome,
393 respectively; pairwise Wilcoxon tests revealed no significant differences in repetitive sequence
394 densities. We found no difference in TE family proportions between these regions either (Figure S2B).
395 Repetitive sequence density was significantly higher in stratum 2 than in stratum 3 (*p*-value for a
396 pairwise Wilcoxon test = 0.0053 with FDR correction). We found no genes with a d_N/d_S ratio >1 in the
397 non-recombining region, i.e. with higher non-synonymous than synonymous substitution rates (the
398 mean d_N/d_S was 0.11 for genes with positive d_S values). As noted above, we found no evidence for

399 genomic rearrangements between the two mating-type chromosomes in the non-recombining region
400 (Figure 3B).

401

402 ***Validation of the region without recombination by progeny analysis***

403 We investigated the lack of recombination in the heterozygous region around the mating-type locus in
404 the CBS815.71 strain. We obtained offspring resulting from a selfing event in the CBS815.71 strain,
405 *i.e.,* a cross between CBS815.71-sp3 and CBS815.71-sp6. We genotyped 107 offspring resulting
406 from haploid spores isolated from five-spore asci (i.e., asci with three large dikaryotic spores and two
407 small monokaryotic spores; Figure 1). We initially used two genetic markers, one at each end of the
408 heterozygous region, and then three additional markers in the three recombinant offspring to delimit
409 more finely the regions in which recombination events occurred (Figure S7). We detected no
410 recombination events at the edge of stratum 3 (*i.e*., between the *P_NRR2* marker and the mating-type
411 locus) but we found recombination events at the edge of stratum 2 (between the markers *P_NRR4*
412 and *P_NRR5*) in three of the 107 offspring. We found no recombination event between the mating-
413 type locus and the additional markers *P_NRR7*, *P_NRR6* and *P_NRR5* located 0.808 Mb, 1.054 Mb
414 and 1.088 Mb from the mating-type locus, respectively. Given the position of the MAT locus, this
415 suggests a complete lack of recombination over a 1.3 Mb region in strata 1 and 3, and in a large part
416 of stratum 2, as recombination occurred only at the edge of this stratum. Stratum 2 is, therefore, likely
417 slightly smaller than the heterozygous region in the CBS815.71 strain, the heterozygosity at its edge
418 probably resulting from an outcrossing event a few generations ago.

419

420 ***Orthologs in the non-recombining regions across* Sordariales**

421 We aimed at investigating gene orthology relationships and synteny between the non-recombining
422 regions on the mating-type chromosomes of the three pseudo-homothallic species, *S. tetrasporum*, *P.*
423 *anserina* and *N. tetrasperma.* However, several rearrangements occurred following recombination
424 suppression on the mating-type chromosomes in *N. tetrasperma.* We therefore used the genome of
425 the closely related heterothallic *N. crassa* species instead, as a proxy for the ancestral gene order in
426 *N. tetrasperma* before recombination suppression. No recombination suppression around the mating-
427 type locus has been reported in *N. crassa* (26,49). This analysis therefore also provided an

428 opportunity for an interesting contrast with species displaying recombination suppression. In an
429 analysis of single-copy orthologs, we found that the mating-type chromosomes, and all the other
430 chromosomes, displayed regions of synteny, but also breaks of synteny between species, and
431 mesosynteny, *i.e.,* a global conservation of gene content despite rearrangements in order and
432 orientation (Figure 5A; Figure S8), as expected given their phylogenetic distance (50). In particular, 69
433 orthologs common to the species studied and belonging to stratum 3 of *S. tetrasporum* had a well-
434 conserved gene order in a 300 kb region around the mating-type locus (Figure 5A), suggesting some
435 conservation of the ancestral gene order in the region around the mating-type locus in these distantly
436 related pseudo-homothallic species, and in other non-pseudo-homothallic Sordariales, as previously
437 reported (32). The region around the putative centromere identified on the *S. tetrasporum* mating-type
438 chromosome had orthologous genes and gene orders conserved with the *P. anserina* and *N. crassa*
439 centromeric region over a distance of 700 kb despite an inversion, providing support for the putative
440 location of the centromere on the *S. tetrasporum* mating-type chromosome identified above (Figure
441 5A).

442 We also found conserved gene content and synteny between parts of the non-recombining
443 regions in the three species despite rearrangements. In *S. tetrasporum*, 261 of the 406 genes located
444 in the identified region of suppressed recombination around the mating-type locus had orthologous
445 genes in both *P. anserina* and *N. crassa.* We found that 138 of these 261 genes were also located in
446 the region of suppressed recombination around the mating-type locus in the *P. anserina* S strain
447 (Figure 5B). Most of these shared genes (85%) were part of stratum 3, encompassing the mating-type
448 locus, and stratum 1, the oldest evolutionary stratum in *S. tetrasporum* (Figure 5A(2),5B). No
449 evolutionary strata have previously been identified in *P. anserina*, but the oldest evolutionary stratum
450 in *P. pseudocomata,* a cryptic species closely related to *P. anserina* (27), was orthologous to stratum
451 3 in *S. tetrasporum*. Most genes (82%) of stratum 2 in *S. tetrasporum* had orthologs in *P. anserina* in
452 the recombining region between the mating-type locus and the centromere (Figure 5A(ii) & 5B). The
453 region of recombination suppression was located from the mating-type locus in the direction of the
454 telomere in *S. tetrasporum*, whereas it was located from the mating-type locus in the direction of the
455 centromere in *P. anserina* and other species of the *P. anserina* species complex (Figure 5A(ii)&5B).
456 The distance between the centromere and the mating-type locus was 1.1 Mb in *S. tetrasporum* and
457 2.9 Mb in *P. anserina.*

458 We further found that 188 of the 406 genes in the non-recombining region of *S. tetrasporum,*
459 (mostly in strata 3 and 2) were also present in the non-recombining region in *N. tetrasperma* (Figure
460 5B), with the genes from *S. tetrasporum* stratum 1 present in the flanking region of the non-
461 recombining region in *N. tetrasperma.* In total, 90 genes were common to the non-recombining
462 regions of the three pseudo-homothallic species, including genes at the two edges of these non-
463 recombining regions (Figure 5A). The predicted functions of these 90 orthologs, when available, did
464 not appear to be related to mating or mating-type functions (Table S4).
465
466 **DISCUSSION**
467
468 ***Striking evolutionary convergence***
469 This study of the breeding system and sexual biology of the little-studied pseudo-homothallic fungus
470 *S. tetrasporum* reveals a striking convergence with *P. anserina* and other cryptic species of the *P.*
471 *anserina* complex, for multiple ecological and reproductive traits. These two distantly related fungi
472 thrive in herbivore dung and produce predominantly dikaryotic spores carrying opposite mating types.
473 In both cases, this is due to mating-type segregation during the second meiotic division associated
474 with a single systematic CO event between the centromere and the mating-type locus. In addition,
475 both *S. tetrasporum* and *P. anserina* display recombination suppression around this locus ((23) and
476 this study). We found that recombination suppression had expanded in several successive steps in *S.*
477 *tetrasporum*, as in *P. peudocomata,* which belongs to the *P. anserina* species complex (27). The
478 association between pseudo-homothallism (self-fertile dikaryotic spores), recombination suppression
479 around the mating-type locus and evolutionary strata also evolved independently in the *N.*
480 *tetrasperma* complex, representing an additional case of convergence. However, unlike *S.*
481 *tetrasporum* and *P. anserina, N. tetrasperma* displays recombination suppression up to the
482 centromere and mating-type segregation during the first meiotic division (26,48).
483
484 ***Association between pseudo-homothallism and recombination suppression: evolutionary and***
485 ***proximal causes***
486 Such a convergent association between recombination suppression and pseudo-homothallism (with
487 the production of heterokaryotic spores carrying both mating types and growth as a heterokaryotic

488 mycelium rather than as a homokaryon in the predominant phase of the lifecycle, as in most
489 ascomycetes) suggests causal relationships. Suppression of recombination around the mating-type
490 locus may be selected for if it favors the production of heterokaryotic ascospores, thus facilitating the
491 compaction of nuclei of opposite mating types in dispersing spores under the particular pattern of
492 meiotic segregation. The resulting self-fertile heterokaryotic ascospores allow reproductive insurance
493 in short-lived habitats such as dung. However, the occurrence of a CO between the centromere and
494 the proximal end of the region of suppressed recombination in almost all meiosis I to cause mating-
495 type segregation during the second meiotic division still calls for an explanation. Indeed, if we
496 consider the 21 ± 3 COs occurring at each meiosis in one nucleus of *Sordaria macrospora* (51,52) as
497 a proxy for the number of COs occurring in *S. tetrasporum* displaying approximately the same
498 genome size, and if we take into account the number of obligate COs occurring on each of the seven
499 chromosomes, we can estimate that 11 to 17 COs remain to be randomly distributed across a
500 genome of 32 Mbp. It is therefore unlikely that one CO takes place between the centromere and the
501 mating-type locus in 99.5 % of the meioses in *P. anserina*, the distance between the centromere and
502 the mating-type locus being 2.9 Mbp, and in *S. tetrasporum,* the distance between the centromere
503 and the mating-type locus being 1.2 Mbp. The occurrence of a second CO between the centromere
504 and the mating-type locus should be prevented, as two COs in this region would result in FDS. This
505 second CO might be prevented by positive interference, but this mechanism alone may not be
506 sufficient to reach the very high frequency of SDS.

507 It therefore appears more likely that a yet unidentified mechanism has evolved that enforces
508 the occurrence of the single and systematic CO event between the centromere and the mating-type
509 locus, independently in both *P. anserina* and *S. tetrasporum*, together with a mechanism compacting
510 two nuclei per ascospore, for the production of self-fertile ascospores. Suppression of recombination
511 around the mating-type locus may be directly linked to the mechanism that prevents a second CO
512 around the mating type locus, which would yield FSD instead of SDS. The selective advantage of
513 producing self-fertile spores would then be the driver to develop this mechanism.

514 An alternative hypothesis may be proposed considering that the mating-type locus is always
515 heterozygous in heterokaryons. Indeed, a recent theoretical model showed that recombination
516 suppression capturing a permanently heterozygous locus may be selected due to its capacity to
517 shelter deleterious alleles in organisms with an extended diploid or dikaryotic phase (14). More

518 precisely, recombination suppression may be selected because it protects DNA fragments with fewer
519 deleterious mutations than average in the population, but the load of these mutations will still prove
520 problematic when they become frequent enough to become homozygous; the capture of a
521 permanently heterozygous allele prevents this effect (14). This mechanism can also explain the
522 evolution of successive evolutionary strata, as observed here in *S. tetrasporum* and, previously, in *N.*
523 *tetrasperma* and *P. pseudocomata* (22,27,27,48), the basidiomycete mushroom *Agaricus bisporus*
524 (53) and repeatedly in *Microbotryum* basidiomycete fungi, plant pathogens in natural ecosystems
525 (8,9,18,54). This mechanism may also account for the suppression of recombination in *N.*
526 *tetrasperma*.

527 In this study, we found no detectable differences in growth between homokaryons of the two
528 mating types and the heterokaryon in *S. tetrasporum*, but we found that one of the mating-type alleles
529 was more often lost during mycelial growth. In addition, fitness differences even smaller than those
530 detectable here can promote the evolution of recombination suppression (14), and genes with
531 deleterious alleles may be involved in specific parts of the life cycle not evaluated *in vitro,* and related
532 to the dung habitat or resistance to harsh conditions. We found that 13% of the thalli grown from
533 ascospores *in vitro* ended up homokaryotic, and the mechanism involved could function in
534 haplodiplontic lifecycles, depending on the mean length or frequency of the haploid phase and the
535 strength of selection (14). The mycelia in dung may not grow for long enough for the loss of a nucleus
536 to be occur very often, especially as *S. tetrasporum* is mostly found on small pellets of rabbit dung
537 (unpublished data).

538 The finding that the non-recombining regions in *P. anserina, N. tetrasperma* and *S.*
539 *tetrasporum* contain a number of shared orthologous genes, particularly at the two edges of the non-
540 recombining region, and that these regions display some level of synteny, raises the possibility of a
541 third hypothesis: the selection of recombination suppression to maintain beneficial allelic combinations
542 (55), as observed for supergenes in plants and animals (56,57). No function known to be directly
543 related to mating compatibility was found among these orthologous genes, except for the mating-type
544 locus, but several genes involved in sexual development in *P. anserina* are located in the non-
545 recombining regions in both *P. anserina* (23) and *S. tetrasporum* (this study): *ami1*, controlling nuclear
546 migration events (44) and *PaRID*, a RID-like putative cytosine methyltransferase that controls sexual
547 development (45). However, there is no evidence of antagonistic selection between mating types for

548 these functions (23) and we found no phenotypic differences between homokaryons of opposite
549 mating types. Nevertheless, we cannot rule out the possibility that there are differences in other parts
550 of the life cycle not investigated here *in vitro*.

551 These various evolutionary hypotheses for explaining recombination suppression are not
552 mutually exclusive, and the evolutionary causes of recombination suppression may differ between
553 evolutionary strata and species. The proximal (mechanistic) causes of recombination suppression
554 also remain unknown. We detected no chromosomal inversion between mating-type chromosomes in
555 *S. tetrasporum*, as in some other fungi in which recombination is also suppressed close to the mating-
556 type locus without inversion, such as *P. anserina* and other species of the *P. anserina* complex, *N.*
557 *tetrasperma* and *Microbotryum* fungi (8,23,26,27). Histone modification can also prevent
558 recombination (58,59) and this aspect warrants investigation in *S. tetrasporum*. There may also be
559 recombination modifiers in *cis*. The proximal cause for the single CO event between the centromere
560 and the mating-type locus is also unknown. The shorter genomic region between the centromere and
561 the mating-type locus in *S. tetrasporum* (1.2 Mb) than in *P. anserina* (2.9 Mb) makes this species an
562 excellent model for identifying the proximal factors responsible for the single CO event, if they are
563 located in *cis*. The convergent evolution of a single systematic CO event between the mating-type
564 locus and the centromere in these two species provides an opportunity to study the genetic basis of
565 the convergent evolution of this phenomenon.

566

567 ***Evolutionary strata***

568 We detected three evolutionary strata in the CBS815.71 *S. tetrasporum* strain, indicating a stepwise
569 extension of recombination suppression. Our progeny analysis showed that stratum 2 did not cover
570 the entire corresponding heterozygous region, the extremity of the heterozygous region probably
571 being a remnant of an outcrossing event a few generations ago. Nevertheless, the progeny analysis
572 showed that strata 1 and 3, and much of stratum 2, probably display a full suppression of
573 recombination. This gradual progression of recombination suppression cannot be explained by sexual
574 antagonism, as male and female functions are not associated with mating types in fungi (19,60). In
575 addition, monokaryotic ascospores are rare in *S. tetrasporum* and traits and ecological features are
576 similar between mating types, so other types of antagonistic selection are also unlikely. Stepwise
577 recombination suppression in this dikaryotic fungus may have been selected to shelter deleterious

578 alleles (14). It may appear surprising that the most ancient evolutionary stratum, stratum 1, with the
579 highest d_S values, does not encompass the mating-type locus. However, this oldest stratum is very
580 close to the mating-type locus and the deleterious allele sheltering model predicts the possible
581 evolution of recombination suppression at sites tightly linked to but not encompassing the
582 permanently heterozygous locus (14). This situation has, in fact, been observed in the chestnut blight
583 fungus *Cryphonectria parasitica* (61). It is also possible that the most ancient evolutionary stratum
584 encompassed the mating-type locus but that the limits of the stratum were obscured by subsequent
585 gene conversion events. Alternatively, the different strata may correspond to gradual increases in the
586 SDS frequency, by stepwise increase of the efficiency of the mechanism preventing a second CO in
587 the region of mating-type locus and FDS. The selective pressure for this stepwise increase would be
588 to reach a higher number of dikaryotic ascospores growing into self-fertile mycelia.
589
590 ***No sign of degeneration in the non-recombining region***
591 We found no enrichment in repeats, rearrangements or non-synonymous substitutions, whereas
592 transposable elements, non-synonymous substitutions and non-optimal codon usage have all been
593 found to increase with time since recombination suppression in the mating-type chromosomes of
594 *Microbotryum* anther-smut fungi (9,54,62). Gene disruptions due to small indels remain to be
595 investigated. The suppression of recombination may have occurred too recently in *S. tetrasporum*, or
596 recombination or gene conversion may occur occasionally, as suggested in *P. anserina* (27). The low
597 d_S values in the center of the non-recombining region, between strata 1 and 2, suggests that gene
598 conversion may occur, as observed in the non-recombining regions of mating-type chromosomes in
599 other fungi (8,9,23,63). We found no footprints of RIP, the fungal genome defense mechanism that
600 introduces cytosine-to-thymine transitions into repetitive sequences to control transposable elements
601 (38,39). Nevertheless, the TE load was not high in *S. tetrasporum*, suggesting that this fungus may
602 have evolved another mechanism of transposable element control, such as RNA silencing (64).
603
604 ***Mating system in* Schizothecium tetrasporum**
605 We found a higher percentage of homokaryotic thalli resulting from ascospore germination in *S.*
606 *tetrasporum* than in *P. anserina* (13% versus 1%). Homokaryons may be recovered due to first-
607 division segregation, the loss of one nucleus after germination or a particular pattern of nucleus

608 migration following the post-meiosis mitosis. We found that nuclei could be lost during vegetative
609 growth *in vitro* in *S. tetrasporum* (here in 13% of the germinating ascospores), whereas this is not the
610 case in *P. anserina* (47), suggesting that *S. tetrasporum* may sometimes, albeit rarely, end up
611 homokaryotic in nature. Such nucleus losses may be due to active competition between nuclei
612 (65,66) or the presence of deleterious alleles associated with a mating type. The occurrence of
613 mycelia of a single mating type could promote some degree of outcrossing, which could be checked in
614 analyses of the levels of heterozygosity of dikaryons in natural populations. Nevertheless, the rate of
615 self-fertile (heterokaryotic) ascospores was high, and this would be expected to promote a high level
616 of selfing. Population genomics approaches detected widespread genome-wide homozygosity in
617 dikaryons of *P. anserina*, indicating high selfing rates, but with occasional stretches of heterozygosity,
618 also indicating the occurrence of outcrossing in nature (27,67,68). The optimal media and conditions
619 for vegetative growth and sexual reproduction identified here will facilitate further investigations of the
620 lifecycle and biology of *S. tetrasporum*. The reference strain was found to be highly homozygous, as
621 expected under high rates of selfing. If we assume that the non-recombining region evolved to prevent
622 a second CO, to maximize the frequency of SDS and thereby of self-fertile spores, it may appear
623 intriguing that no mechanism evolved to subsequently maintain a dikaryotic mycelium, as for instance
624 the crozier cells that are present in the perithecia and are analogous to the dikaryotic clamp cells of
625 Basidiomycetes (69). It may be that, in nature, the mycelium does not grow long enough to frequently
626 loose a nucleus or that the occurrence of mycelia carrying a single mating type is beneficial in
627 promoting outcrossing, as does the formation of a few asci with 5 ascospores including two
628 monokaryotic ascospores.
629
630 ***Conclusion***
631 In conclusion, we found a striking convergence in lifecycle, sexual biology and stepwise
632 recombination suppression around the mating-type locus in phylogenetically distant fungi of the order
633 Sordariales. Documenting convergent evolution is important, as it shows that evolution can be
634 repeatable, and not only contingent (70). Studies of these traits in additional species would make it
635 possible to perform a more robust assessment of the degree of convergence in trait association and,
636 thus, of the causal relationship. Furthermore, the broad convergence towards an association between
637 dikaryotic life cycle and stepwise recombination suppression beyond the mating-type locus despite

638 the lack of sexual antagonism provides support for alternative hypotheses, such as deleterious allele
639 sheltering, as an explanation for the suppression of recombination beyond mating-type or sex-
640 determining alleles (14).
641
642
643 **MATERIALS AND METHODS**
644
645 **Strain origins, experimental crosses and culture**
646 The dikaryotic strain CBS815.71 of *S. tetrasporum* was obtained from the Centraalbureau voor
647 Schimmelcultures (CBS). No optimized methods have been described for culturing *S. tetrasporum*
648 and inducing sexual reproduction in this species. We therefore tested several media, to select those
649 optimal for growth and sexual reproduction (M2, M3, Oat Meal Agar and V8 agar; (71)), and for
650 ascospore germination (the same media plus *P. anserina* germination medium (G), (71)). Growth and
651 sexual reproduction were optimal on V8 medium (composition per liter: 15 g agar, 2 g $CaCO_3$, 200 mL
652 *V8* tomato juice and 800 mL water) at 22°C with 12 h of illumination. Incubation at a higher
653 temperature, such as 26°C, often resulted in aborted fruiting bodies. Growth and ascospore recovery
654 were very slow at lower temperatures (*e.g.*, 18°C). We observed 100% germination on G medium
655 (composition per liter: 4.4 g ammonium acetate, 15 g bactopeptone and 13 g agar) with a 65°C heat
656 shock for 30 minutes just after the plating of ascospores. On all the other media tested, germination
657 rates were lower, with no germination in the absence of a heat shock. In optimal conditions, mature
658 perithecia ejecting ascospores were obtained three weeks after inoculation on V8 medium, and
659 germination occurred overnight on G medium after a heat shock. Ascospores could be collected and
660 plated with the same methods as used for *P. anserina* (71).
661 In these optimal conditions, we generated and isolated two F1 monokaryotic strains by
662 inducing a sexual cycle in the self-fertile heterokaryotic culture received from CBS815.71: the
663 CBS815.71-sp3 strain with a mating-type allele orthologous to the *mat+* mating type of *Podospora*
664 *anserina*, corresponding to the *MAT1-1* allele according to the official nomenclature (34), and the
665 CBS815.71-sp6 strain with a mating-type allele orthologous to the *mat-* mating type of *P. anserina*,
666 corresponding to the *MAT1-2* allele according to the official nomenclature (34). We assessed the
667 frequency of second-division segregation (SDS) at the mating-type locus and, therefore, the

668 frequency of heterokaryotic spore formation, by generating and isolating 190 four-spore asci from a
669 cross between CBS815.71-sp3 and CBS815.71-sp6. We studied the size of the region in which
670 recombination was fully abolished around the mating-type locus, by isolating 107 small ascospores
671 from five-spore asci (monokaryotic) from a cross between CBS815.71-sp3 and CBS815.71-sp6. After
672 isolation, the strains were maintained on M2 minimal medium to prevent contamination (71), and were
673 incubated at 22°C for growth. The growth of CBS815.71-sp3 and CBS815.71-sp6 homokaryons and
674 the CBS815.71 dikaryotic strain was assessed on OA, V8 and M2 media (71). The diameter of
675 mycelial colonies was measured after 3 and 10 days of growth at 22°C with 12 h illumination, with a
676 10 cm ruler. Mean growth rate per day was calculated over the seven-day period from day 3 to day
677 10. Dry weights were measured after 10 days of growth in liquid M2 medium (50 mL); the mycelium
678 was filtered and dried at 65°C overnight. Measurements were performed on five Petri dishes for each
679 strain and each medium. ANOVA was performed with R software v 4.2.0.
680
681 **Genome sequencing and other genomic data**
682 We generated long read-based genome assemblies by sequencing the genomes of the *S.*
683 *tetrasporum* strains CBS815.71-sp3 and CBS815.71-sp6 with both Illumina technology on the
684 HiSeq2500 platform (150 bp long paired-end reads) and Oxford Nanopore MinION technology with an
685 R9 flow cell. For each DNA extraction, we prepared 100–200 mg aliquots of mycelium, which were
686 stored in a 1.5 mL Eppendorf tube at -80°C for at least 24 hours before lyophilization. A sheet of
687 cellophane was placed over the M2 medium before inoculation with spores, such that the mycelium
688 grew on the cellophane for three to four days and could be scraped off easily. For Illumina
689 sequencing, DNA was extracted with the commercial Nucleospin Soil kit from Macherey Nagel.
690 Illumina library preparation and genome sequencing were outsourced to the sequencing core facility
691 of Genoscope (last accessed May 15, 2021). For Nanopore sequencing, mycelium DNA was
692 extracted with the NucleoBond High Molecular Weight DNA kit from Macherey-Nagel, with the
693 mechanical disruption of about 30 mg of lyophilized mycelium with beads for 5 min at 30 Hz. The
694 Nanopore library was prepared with the SQK-LSK109 ligation sequencing kit, and sequencing was
695 performed in house. The quality of the raw reads was analyzed with fastQC 0.11.9 (72) for the
696 Illumina raw reads and pycoQC 2.5.0.23 (73) for the Nanopore raw reads (Table S5).

697 In addition, the genome and transcriptome of *S. tetrasporum* strain CBS815.71-sp3 were
698 sequenced with Illumina technology by the Joint Genome Institute (JGI). DNA was extracted following
699 (74) from mycelium grown on cellophane-covered potato dextrose agar medium. Plate-based DNA
700 library was prepared for Illumina sequencing on the PerkinElmer Sciclone NGS robotic liquid handling
701 system with the Kapa Biosystems library preparation kit. Sample DNA (200 ng) was sheared into 600
702 bp fragments with a Covaris LE220 focused ultrasonicator. The sheared DNA fragments were size-
703 selected by double-SPRI and the selected fragments were end-repaired, A-tailed, and ligated with
704 Illumina-compatible sequencing adaptors from IDT containing a unique molecular index barcode. RNA
705 was extracted from the same mycelial colonies as DNA using TRIzol (Invitrogen) following
706 manufacturer's instructions (https://assets.thermofisher.com/TFS-
707 Assets/LSG/manuals/trizol_reagent.pdf). Plate-based RNA sample preparation was obtained with the
708 PerkinElmer Sciclone NGS robotic liquid handling system and the Illumina TruSeq Stranded mRNA
709 HT sample preparation kit, with the poly-A selection of mRNA according to the protocol in the Illumina
710 user guide (https://support.illumina.com/sequencing/sequencing_kits/truseq-stranded-mrna.html),
711 under the following conditions: 1 µg total RNA as the starting material, and eight PCR cycles for
712 library amplification. The prepared libraries were then quantified with the KAPA Biosystem next-
713 generation sequencing library qPCR kit (Roche) and a Roche LightCycler 480 real-time PCR
714 instrument. The quantified libraries were then then multiplexed with other libraries, and the pool of
715 libraries was prepared for sequencing on the Illumina NovaSeq 6000 sequencing platform with
716 NovaSeq XP v1.5 reagent kits, an S4 flow cell, following a 2x150 indexed run method. All raw Illumina
717 sequence data were filtered for artifacts/process contamination. DNA reads produced by the JGI were
718 then assembled with SPAdes v3.15.2 (75). The obtained genome assembly is referred to as the
719 Illumina read-based assembly of CBS815.71-sp3.
720 The genome of the *P. anserina* S *mat*+ strain "Podan2" (32) was downloaded from the JGI
721 MycoCosm website (https://mycocosm.jgi.doe.gov/mycocosm/home, last accessed November 15,
722 2018) and improved annotations by (76) were downloaded from the GitHub repository,
723 https://github.com/johannessonlab/SpokBlockPaper (last accessed June 1, 2020). The genome of the
724 OR74A *N. crassa mat A* strain (77) was downloaded from GenBank under accession number
725 GCA_000182925.2 (last accessed May 10, 2022).
726

727 **Long read-based genome assemblies for CBS815.71 strains**

728 *De novo* assemblies of the genomes of the CBS815.71-sp3 and CBS815.71-sp6 strains were
729 constructed from both Illumina reads produced at Genoscope and Nanopore reads. For each
730 genome, the raw Nanopore reads were trimmed and assembled with Canu v1.8 (78) with the option
731 genomeSize=35m. The assembly obtained with Canu was polished twice with Nanopore trimmed
732 reads using first Racon v1.4.3 (79) with the options m=8 x=6 g=8 w=500 and then with medaka
733 (https://github.com/nanoporetech/medaka) with the default settings. The assembly obtained was
734 polished five times with the trimmed Illumina reads with Pilon v1.24 (80). For each round of polishing,
735 BWA v0.7.17 (81) was used to align the Nanopore or Illumina trimmed reads with the assembly for
736 polishing. The Illumina reads were first trimmed with Trimmomatic v0.36 (82) with the options:
737 ILLUMINACLIP:TruSeq3-PE.fa:2:30:10 LEADING:10 TRAILING:10 SLIDINGWINDOW:5:10
738 MINLEN:50. The quality of the final assemblies was assessed with Quast v5.1 (83). We checked for
739 contamination, by performing a BLAST analysis of the assembly scaffolds against the online NCBI
740 nucleotide collection database (https://blast.ncbi.nlm.nih.gov/, last accessed March 5, 2022) and
741 looking at the coverage of Illumina and Nanopore reads on the final assemblies. We also evaluated
742 the completeness of the final assemblies with BUSCO v5.2.2 (84,85) and the Sordariomyceta
743 ortholog set (sordariomycetes_odb10, 2020-08-05, *n*= 3817 orthologous groups searched). We also
744 ran BUSCO analysis on the Podan2 *P. anserina* assembly for comparison.

745

746 **Genome annotation**

747 Before gene annotation, the final assemblies were formatted (contigs were renamed and ordered in
748 descending order of size) and masked for repeats with RepeatMasker (86) and the funnannotate
749 v1.8.9 pipeline (87). We performed gene annotation on the masked assemblies with BRAKER v2.1.6,
750 which uses a combination of the *ab initio* gene predictors Augustus and GeneMark-ET (88). We ran
751 BRAKER twice, first using the BUSCO dataset of proteins sordariomycetes_odb10 (84) as evidence,
752 and then using the RNAseq dataset as evidence. We optimized the training steps, by concatenating
753 the two homokaryotic genomes derived from the same heterokaryotic strain, CBS815.71, into a single
754 fasta file and running BRAKER on the combined fasta file. For RNAseq mapping, we used STAR
755 v2.7.10a (89) with the default settings. We combined the results of the two BRAKER runs with
756 TSEBRA (the Transcript Selector for BRAKER; https://github.com/Gaius-Augustus/TSEBRA), with the

757 option 'intron_support' set to 0.2. We ran InterProScan5 v5.54-87.0 (90), TMHMM v2.0c (91), SignalP
758 v4.1 (92) and Phobius (93) and obtained predicted protein annotations from PFAM, InterPro, EggNog,
759 UniProtKB, MEROPS, CAZyme, and GO ontology. For repeat annotation, we performed a *de novo*
760 identification of transposable elements in the final assemblies with RepeatModeler v1.0.11 (94). We
761 merged the consensus sequences obtained wiereth the RepBase library available in RepeatMasker
762 v4.0.9 (86) and the custom library "PodoTE-1.00" built for the *Podospora anserina* species complex
763 by (95) and the *Neurospora* library of (96) "Gioti_neurospora_repeats.renamed" (both available from
764 the GitHub repository https://github.com/johannessonlab/SpokBlockPaper, last accessed June 1,
765 2020). We used RepeatMasker v4.0.9 (86) to annotate repeats. We parsed the RepeatMasker
766 outputs and removed low-complexity and simple repeats with the parseRM_merge_interrupted.pl
767 script from https://github.com/4ureliek/Parsing-RepeatMasker-Outputs (last accessed February 25,
768 2021). We retained only TEs longer than 150 bp, and overlapping TEs annotated as belonging to the
769 same family were merged into single elements for the final annotation. We used the TE annotation
770 suggested by (97) to sort TEs by family. We looked for signatures of RIP with the RIPper platform
771 http://theripper.hawk.rocks (default settings; (98)). The mating-type locus was identified by tBLASTn,
772 with the *mat+* and *mat-* idiomorphs of *P. anserina* as queries. The *SMR1*, *SMR2*, *FMR1*, *FPR1* gene
773 models were manually curated as previously described (99), in Artemis v18.0.2 (100). The sequences
774 of proteins containing a MATα_HMG domain were downloaded from the European Nucleotide Archive
775 (ENA) database with accession numbers CDN29981 and ESA43845 for *P. anserina* and *N. crassa*,
776 respectively. Proteins were aligned with Clustal Omega (101) and the alignments were color-coded
777 with JALVIEW v2 (102).
778
779 **Comparative genomics and statistical analyses**
780 For all comparative genomics analyses, we identified orthologous groups with OrthoFinder v2.3.7
781 (103). We calculated d_S values by studying one-to-one orthologs between the CBS815.71-sp3 and
782 CBS815.71-sp6 genome assemblies and retaining only those orthologs with the same number of
783 exons and the same transcript length as predicted. We aligned orthologous gene coding sequences,
784 using the codon-based approach implemented in translatorX v1.1 with default parameters (104). We
785 used the nucleotide alignment as input for the yn00 program in the PAML v.4.9 package (105,106).
786 Pairwise Wilcoxon tests were performed in R with false discovery rate correction. We excluded the

787 four genes located at the edges of strata to assess the differences in d_S between strata. We studied
788 synteny between assemblies, by investigating either collinearity between one-to-one orthologs or
789 running the genome sequence aligner nucmer from MUMmer v4.0.0rc1 (107) with default options. For
790 the identification of small indels between the long-read assemblies, we first aligned the CBS815.71-
791 sp6 genome assembly with the CBS815.71-sp3 genome assembly using Minimap2 (108) with the -cx
792 asm10 -t8 options. We then used samtools mpileup (109) with the following options: -d 250 -m 1 -E --
793 BCF --output-tags DP,DV,DP4,SP.
794
795 **Genotyping of the mating-type locus alleles and surrounding regions**
796 We devised a new method of DNA extraction for genotyping based on a published protocol (110).
797 Briefly, 1 mm^3 plugs were taken directly from cultures growing on agar plates and ground with 200 µL
798 extraction buffer, heated at 95°C for 15 minutes, placed on ice for one minute, briefly vortexed and
799 centrifuged at 15,900 x g for 30 seconds. We determined the mating-type allele of the offspring from a
800 cross between CBS815.71-sp3 and CBS815.71-sp6 by PCR with the primers and conditions
801 described in Table S6 and Table S7. Primers were designed with Primer3 software (111,112), based
802 on the mating-type locus region annotated in the two genome assemblies obtained for *S. tetrasporum.*
803 We visualized amplicons by agarose-gel electrophoresis.
804
805
806 **Data availability**
807 All genomic data produced by the JGI are available from the JGI MycoCosm website
808 (https://mycocosm.jgi.doe.gov/mycocosm/home, last accessed February 5, 2022). The raw Illumina
809 and Nanopore reads and the long read-based assemblies for the CBS815.71-sp3 and CBS815.71-
810 sp6 genomes were deposited in GenBank under the BioProject accession number PRJNAXXX
811 (BioSample ID: xxx, assembly accession number: xxx; available upon publication).
812
813
814 **Acknowledgements**

This work was supported by the Louis D. Foundation award and EvolSexChrom ERC advanced grant #832352 to T.G. and DOE-JGI CSP grant #504394 to P.G. and P.S. We are grateful to J.P. Vernadet for sharing the conda environment to run the BRAKER pipeline.

Author contributions

T.G., F.E.H. and P.S. conceptualized the study, acquired funding and supervised the study. N.V., A.S., V.G., E.D.F., E.L., F.E.H., and P.S. contributed to experiments. N.V., F.E.H., R.D., C.L., P.S. and R.R.d.l.V. analyzed the genomes. N.V., V.G., E.D.F., E.L. and P.S. analyzed the progenies. P.G., S.G., Y. Z., S. T. and I.G. provided RNAseq data and the Illumina based-genome assembly of the CBS815.71-sp3 strains. N.V., F.E.H., P.S., and T.G. wrote the manuscript draft. All authors edited the manuscript.

REFERENCES

1. Muller HJ. Some genetic aspects of sex. Am Nat. 1932 Mar 1;66(703):118–38.

2. Hill WG, Robertson A. The effect of linkage on limits to artificial selection. Genet Res. 1966 Dec;8(3):269–94.

3. Uyenoyama MK. Evolution under tight linkage to mating type. New Phytol. 2005;165(1):63–70.

4. Hartmann FE, Duhamel M, Carpentier F, Hood ME, Foulongne-Oriol M, Silar P, et al. Recombination suppression and evolutionary strata around mating-type loci in fungi: documenting patterns and understanding evolutionary and mechanistic causes. New Phytol. 2021;229(5):2470–91.

5. Goubet PM, Bergès H, Bellec A, Prat E, Helmstetter N, Mangenot S, et al. Contrasted patterns of molecular evolution in dominant and recessive self-incompatibility haplotypes in *Arabidopsis*. PLOS Genet. 2012 Mar 22;8(3):e1002495.

6. Coelho MA, Bakkeren G, Sun S, Hood ME, Giraud T. Fungal sex: The Basidiomycota. Microbiol Spectr. 2017 Jun;5(3):FUNK-0046-2016.

7. Bergero R, Charlesworth D. The evolution of restricted recombination in sex chromosomes. Trends Ecol Evol. 2009 Feb 1;24(2):94–102.

8. Branco S, Carpentier F, Rodríguez de la Vega RC, Badouin H, Snirc A, Prieur SL, et al. Multiple convergent supergene evolution events in mating-type chromosomes. Nat Commun. 2018 May 21;9(1):2000.

9. Branco S, Badouin H, Rodríguez de la Vega RC, Gouzy J, Carpentier F, Aguileta G, et al. Evolutionary strata on young mating-type chromosomes despite the lack of sexual antagonism. Proc Natl Acad Sci. 2017 Mar 7;114(27):7067–72.

10. Hartmann FE, Duhamel M, Carpentier F, Hood ME, Foulongne-Oriol M, Silar P, et al. Recombination suppression and evolutionary strata around mating-type loci in fungi: documenting patterns and understanding evolutionary and mechanistic causes. New Phytol. 2021;229(5):2470–91.

11. Ironside JE. No amicable divorce? Challenging the notion that sexual antagonism drives sex chromosome evolution. BioEssays. 2010 Aug 1;32(8):718–26.

12. Charlesworth. The status of supergenes in the 21st century: recombination suppression in Batesian mimicry and sex chromosomes and other complex adaptations. Evol Appl. 2016;9(1):74–90.

13. Bazzicalupo AL, Carpentier F, Otto SP, Giraud T. Little evidence of antagonistic selection in the evolutionary strata of fungal mating-type chromosomes (*Microbotryum lychnidis-dioicae*). G3 Genes Genomes Genet. 2019 Jun 1;9(6):1987–98.

14. Jay P, Tezenas E, Véber A, Giraud T. Modeling the stepwise extension of recombination suppression on sex chromosomes and other supergenes through deleterious mutation sheltering. PLOS Biol. 2022 in press. available at https://www.biorxiv.org/content/10.1101/2021.05.17.444504v2.full.pdf

15. Lenormand T, Roze D. Y recombination arrest and degeneration in the absence of sexual dimorphism. Science. 2022 Feb 11;375(6581):663–6.

16. Kent TV, Uzunović J, Wright SI. Coevolution between transposable elements and recombination. Philos Trans R Soc B Biol Sci. 2017 Dec 19;372(1736):20160458.

17. Gladieux P, Ropars J, Badouin H, Branca A, Aguileta G, de Vienne DM, et al. Fungal evolutionary genomics provides insight into the mechanisms of adaptive divergence in eukaryotes. Mol Ecol. 2014 Feb 1;23(4):753–73.

18. Duhamel M, Carpentier F, Begerow D, Hood ME, Rodríguez de la Vega RC, Giraud T. Onset and stepwise extensions of recombination suppression are common in mating-type chromosomes of *Microbotryum* anther-smut fungi. J Evol Biol. Available from: https://onlinelibrary.wiley.com/doi/abs/10.1111/jeb.13991

19. Billiard, López-Villavicencio M, Hood ME, Giraud T. Sex, outcrossing and mating types: unsolved questions in fungi and beyond. J Evol Biol. 2012;25(6):1020–38.

20. Dyer PS, Inderbitzin P, Debuchy R. 14 mating-type structure, function, regulation and evolution in the Pezizomycotina. In: Wendland J, editor. Growth, Differentiation and Sexuality. Cham: Springer International Publishing; 2016. p. 351–85. (The Mycota). Available from: https://doi.org/10.1007/978-3-319-25844-7_14

21. Raju NB, Perkins DD. Diverse programs of ascus development in pseudohomothallic species of *Neurospora*, *Gelasinospora*, and *Podospora*. Dev Genet. 1994;15(1):104–18.

22. Menkis A, Jacobson DJ, Gustafsson T, Johannesson H. The mating-type chromosome in the filamentous ascomycete *Neurospora tetrasperma* represents a model for early evolution of sex chromosomes. PLOS Genet. 2008 Mar 14;4(3):e1000030.

23. Grognet P, Bidard F, Kuchly C, Tong LCH, Coppin E, Benkhali JA, et al. Maintaining two mating types: structure of the mating type locus and its role in heterokaryosis in *Podospora anserina*. Genetics. 2014 May 1;197(1):421–32.

24. Boucher C, Nguyen TS, Silar P. Species delimitation in the *Podospora anserina*/*p. paucisetal*/*p. comata* species complex (Sordariales). Cryptogam Mycol. 2017 Dec;38(4):485–506.

25. Corcoran P, Dettman JR, Sun Y, Luque EM, Corrochano LM, Taylor JW, et al. A global multilocus analysis of the model fungus *Neurospora* reveals a single recent origin of a novel genetic system. Mol Phylogenet Evol. 2014 Sep 1;78:136–47.

26. Sun Y, Svedberg J, Hiltunen M, Corcoran P, Johannesson H. Large-scale suppression of recombination predates genomic rearrangements in *Neurospora tetrasperma*. Nat Commun. 2017 Oct 26;8(1):1–8.

27. Hartmann FE, Ament-Velásquez SL, Vogan AA, Gautier V, Le Prieur S, Berramdane M, et al. Size variation of the nonrecombining region on the mating-type chromosomes in the fungal *Podospora anserina* species complex. Mol Biol Evol. 2021 Jun 1;38(6):2475–92.

28. Heslot H. Contribution à l'étude cytogénétique et génétique des Sordariacées. 1958.

29. Marin-Felix Y, Miller AN, Cano-Lira JF, Guarro J, García D, Stadler M, et al. Re-evaluation of the order Sordariales: Delimitation of Lasiosphaeriaceae s. str., and introduction of the new families Diplogelasinosporaceae, Naviculisporaceae, and Schizotheciaceae. Microorganisms. 2020 Sep 17;8(9):E1430.

30. Huang SK, Hyde KD, Mapook A, Maharachchikumbura SSN, Bhat JD, McKenzie EHC, et al. Taxonomic studies of some often over-looked Diaporthomycetidae and Sordariomycetidae. Fungal Divers. 2021 Nov 1;111(1):443–572.

31. Hyde KD, Maharachchikumbura SSN, Hongsanan S, Samarakoon MC, Lücking R, Pem D, et al. The ranking of fungi: a tribute to David L. Hawksworth on his 70th birthday. Fungal Divers. 2017 May 1;84(1):1–23.

32. Espagne E, Lespinet O, Malagnac F, Da Silva C, Jaillon O, Porcel BM, et al. The genome sequence of the model ascomycete fungus *Podospora anserina*. Genome Biol. 2008 May 6;9(5):R77.

33. Esser K, Prillinger H. A new technique for using spermatia in the production of mutants in *Podospora*. Mutat Res Mol Mech Mutagen. 1972 Dec 1;16(4):417–9.

34. Turgeon BG, Yoder OC. Proposed nomenclature for mating type genes of filamentous Ascomycetes. Fungal Genet Biol. 2000 Oct 1;31(1):1–5.

35. Marcou D. Notion de longévité et nature cytoplasmique du déterminant de la sénescence chez quelques champignons. Annales des Sciences Naturelles, Botaniques Paris. 1961;Sér. 12, 2: 653-764.

36. Roper M, Simonin A, Hickey PC, Leeder A, Glass NL. Nuclear dynamics in a fungal chimera. Proc Natl Acad Sci U S A. 2013 Aug 6;110(32):12875–80.

37. Barth G. Genetic Maps 1987: a compilation of linkage and reconstruction maps of genetically studied organisms, Volume 4. IX + 755 S. Cold Spring Harbor 1987. Cold Spring Harbor Laboratory. ISBN: 0-87969-303-7. J Basic Microbiol. 1989;29(3):190–190.

38. Cambareri EB, Jensen BC, Schabtach E, Selker EU. Repeat-induced G-C to A-T mutations in *Neurospora*. Science. 1989 Jun 30;244(4912):1571–5.

39. Galagan JE, Selker EU. RIP: the evolutionary cost of genome defense. Trends Genet. 2004 Sep;20(9):417–23.

934 40. Silar P, Barreau C, Debuchy R, Kicka S, Turcq B, Sainsard-Chanet A, et al. Characterization of
935 the genomic organization of the region bordering the centromere of chromosome V of
936 *Podospora anserina* by direct sequencing. Fungal Genet Biol. 2003 Aug 1;39(3):250–63.

937 41. Butler G. The Evolution of MAT: The Ascomycetes. Sex Fungi. 2007 Jan 1;3–18.

938 42. Martin T, Lu SW, Tilbeurgh H van, Ripoll DR, Dixelius C, Turgeon BG, et al. Tracing the origin of
939 the fungal α1 domain places its ancestor in the HMG-Box superfamily: Implication for fungal
940 mating-type evolution. PLOS ONE. 2010 Dec 8;5(12):e15199.

941 43. Hutchinson MI, Powell AJ, Tsang A, O'Toole N, Berka RM, Barry K, et al. Genetics of mating in
942 members of the Chaetomiaceae as revealed by experimental and genomic characterization of
943 reproduction in *Myceliophthora heterothallica*. Fungal Genet Biol. 2016 Jan 1;86:9–19.

944 44. Graïa F, Berteaux-Lecellier V, Zickler D, Picard M. *ami1*, an orthologue of the *Aspergillus*
945 *nidulans apsA* gene, is involved in nuclear migration events throughout the life cycle of
946 *Podospora anserina*. Genetics. 2000 Jun 1;155(2):633–46.

947 45. Grognet P, Timpano H, Carlier F, Aït-Benkhali J, Berteaux-Lecellier V, Debuchy R, et al. A RID-
948 like putative cytosine methyltransferase homologue controls sexual development in the fungus
949 *Podospora anserina*. PLOS Genet. 2019 Aug 14;15(8):e1008086.

950 46. Picard-Bennoun M. Does translational ambiguity increase during cell differentiation? FEBS Lett.
951 1982;149(2):167–70.

952 47. Silar P, Picard M. Increased longevity of EF-1 alpha high-fidelity mutants in *Podospora anserina*.
953 J Mol Biol. 1994 Jan 7;235(1):231–6.

954 48. Sun Y, Corcoran P, Menkis A, Whittle CA, Andersson SGE, Johannesson H. Large-scale
955 introgression shapes the evolution of the mating-type chromosomes of the filamentous
956 ascomycete *Neurospora tetrasperma*. PLOS Genet. 2012 Jul 26;8(7):e1002820.

957 49. Ellison CE, Stajich JE, Jacobson DJ, Natvig DO, Lapidus A, Foster B, et al. Massive changes in
958 genome architecture accompany the transition to self-fertility in the filamentous fungus
959 *Neurospora tetrasperma*. Genetics. 2011 Sep 1;189(1):55–69.

960 50. Hane JK, Rouxel T, Howlett BJ, Kema GH, Goodwin SB, Oliver RP. A novel mode of
961 chromosomal evolution peculiar to filamentous Ascomycete fungi. Genome Biol. 2011 May
962 24;12(5):R45.

963 51. Zickler D, Moreau PJ, Huynh AD, Slezec AM. Correlation between pairing initiation sites,
964 recombination nodules and meiotic recombination in *Sordaria macrospora*. Genetics. 1992 Sep
965 1;132(1):135–48.

966 52. Muyt AD, Zhang L, Piolot T, Kleckner N, Espagne E, Zickler D. E3 ligase Hei10: a multifaceted
967 structure-based signaling molecule with roles within and beyond meiosis. Genes Dev. 2014 May
968 15;28(10):1111–23.

969 53. Foulongne-Oriol M, Taskent O, Kües U, Sonnenberg ASM, van Peer AF, Giraud T. Mating-type
970 locus organization and mating-type chromosome differentiation in the bipolar edible button
971 mushroom *Agaricus bisporus*. Genes. 2021 Jul;12(7):1079.

972 54. Carpentier F, Rodríguez de la Vega RC, Jay P, Duhamel M, Shykoff JA, Perlin MH, et al. Tempo
973 of degeneration across independently evolved nonrecombining regions. Mol Biol Evol. 2022 Apr
974 1;39(4):msac060.

975 55. Idnurm A, Hood ME, Johannesson H, Giraud T. Contrasted patterns in mating-type
976 chromosomes in fungi: Hotspots versus coldspots of recombination. Fungal Biol Rev. 2015 Dec
977 1;29(3):220–9.

978 56. Schwander T, Libbrecht R, Keller L. Supergenes and complex phenotypes. Curr Biol. 2014 Mar
979 31;24(7):R288–94.

980 57. Berdan EL, Flatt T, Kozak GM, Lotterhos KE, Wielstra B. Genomic architecture of supergenes:
981 connecting form and function. Philos Trans R Soc B Biol Sci. 2022 Aug;377(1856):20210192.

982 58. Maloisel L, Rossignol JL. Suppression of crossing-over by DNA methylation in *Ascobolus*.
983 Genes Dev. 1998 May 1;12(9):1381–9.

984 59. Ben-Aroya S, Mieczkowski PA, Petes TD, Kupiec M. The compact chromatin structure of a Ty
985 repeated sequence suppresses recombination hotspot activity in *Saccharomyces cerevisiae*.
986 Mol Cell. 2004 Jul 23;15(2):221–31.

987 60. Billiard S, López-Villavicencio M, Devier B, Hood ME, Fairhead C, Giraud T. Having sex, yes,
988 but with whom? Inferences from fungi on the evolution of anisogamy and mating types. Biol
989 Rev. 2011;86(2):421–42.

990 61. Kubisiak TL, Milgroom MG. Markers linked to vegetative incompatibility (*vic*) genes and a region
991 of high heterogeneity and reduced recombination near the mating type locus (*MAT*) in
992 *Cryphonectria parasitica*. Fungal Genet Biol. 2006 Jun 1;43(6):453–63.

993 62. Fontanillas E, Hood ME, Badouin H, Petit E, Barbe V, Gouzy J, et al. Degeneration of the non-
994 recombining regions in the mating-type chromosomes of the anther-smut fungi. Mol Biol Evol.
995 2015;32(4):928–43.

996 63. Sun S, Hsueh YP, Heitman J. Gene conversion occurs within the mating-type locus of
997 *Cryptococcus neoformans* during sexual reproduction. PLoS Genet. 2012 Jul 5;8(7).

998 64. Nakayashiki H. RNA silencing in fungi: Mechanisms and applications. FEBS Lett. 2005 Oct
999 31;579(26):5950–7.

1000 65. Meunier C, Hosseini S, Heidari N, Maryush Z, Johannesson H. Multilevel selection in the
1001 filamentous ascomycete *Neurospora tetrasperma*. Am Nat. 2018 Mar 1;191(3):290–305.

1002 66. Nieuwenhuis BPS, Billiard S, Vuilleumier S, Petit E, Hood ME, Giraud T. Evolution of uni- and
1003 bifactorial sexual compatibility systems in fungi. Heredity. 2013 Dec;111(6):445–55.

1004 67. Corcoran P, Anderson JL, Jacobson DJ, Sun Y, Ni P, Lascoux M, et al. Introgression maintains
1005 the genetic integrity of the mating-type determining chromosome of the fungus *Neurospora*
1006 *tetrasperma*. Genome Res. 2016 Jan 4;26(4):486–98.

1007 68. Ament-Velásquez SL, Vogan AA, Granger-Farbos A, Bastiaans E, Martinossi-Allibert I, Saupe
1008 SJ, et al. Allorecognition genes drive reproductive isolation in *Podospora anserina*. Nat Ecol
1009 Evol. 2022 Jul;6(7):910–23.

1010 69. Coppin E, Berteaux-Lecellier V, Bidard F, Brun S, Ruprich-Robert G, Espagne E, et al.
1011 Systematic deletion of homeobox genes in *Podospora anserina* uncovers their roles in shaping
1012 the fruiting body. PLOS ONE. 2012 May 25;7(5):e37488.

1013 70. Gould S. Wonderful life: the Burgess Shale and the nature of history. WW Norton&Company.
1014 1990.

1015 71. Silar P. Podospora anserina. 2020.

1016 72. Andrews S. FastQC a quality control tool for high throughput sequence data. 2010; Available
1017 from: https://www.bioinformatics.babraham.ac.uk/projects/fastqc/

1018 73. Leger A, Leonardi T. pycoQC, interactive quality control for Oxford Nanopore Sequencing. J
1019 Open Source Softw. 2019 Feb 28;4(34):1236.

1020 74. Thierry M, Charriat F, Milazzo J, Adreit H, Ravel S, Cros-Arteil S, et al. Maintenance of divergent
1021 lineages of the rice blast fungus *Pyricularia oryzae* through niche separation, loss of sex and
1022 post-mating genetic incompatibilities. PLOS Pathogens. 2022 in press. available at
1023 https://www.biorxiv.org/content/10.1101/2020.06.02.129296v4.full.pdf

1024 75. Bankevich A, Nurk S, Antipov D, Gurevich AA, Dvorkin M, Kulikov AS, et al. SPAdes: a new
1025 genome assembly algorithm and its applications to single-cell sequencing. J Comput Biol. 2012
1026 Apr 16;19(5):455–77.

1027 76. Vogan AA, Ament-Velásquez SL, Granger-Farbos A, Svedberg J, Bastiaans E, Debets AJ, et al.
1028 Combinations of *Spok* genes create multiple meiotic drivers in *Podospora*. eLife. 2019;8.

1029 77. Galagan JE, Calvo SE, Borkovich KA, Selker EU, Read ND, Jaffe D, et al. The genome
1030 sequence of the filamentous fungus *Neurospora crassa*. Nature. 2003 Apr;422(6934):859–68.

1031 78. Koren S, Walenz BP, Berlin K, Miller JR, Bergman NH, Phillippy AM. Canu: scalable and
1032 accurate long-read assembly via adaptive k-mer weighting and repeat separation. Genome Res.
1033 2017;27(5):722–36.

1034 79. Vaser R, Sović I, Nagarajan N, Šikić M. Fast and accurate de novo genome assembly from long
1035 uncorrected reads. Genome Res. 2017 May;27(5):737–46.

1036 80. Walker BJ, Abeel T, Shea T, Priest M, Abouelliel A, Sakthikumar S, et al. Pilon: An integrated
1037 tool for comprehensive microbial variant detection and genome assembly improvement. PLOS
1038 ONE. 2014 Nov 19;9(11):e112963.

1039 81. Li H, Durbin R. Fast and accurate short read alignment with Burrows-Wheeler transform.
1040 Bioinforma Oxf Engl. 2009 Jul 15;25(14):1754–60.

1041 82. Bolger AM, Lohse M, Usadel B. Trimmomatic: a flexible trimmer for Illumina sequence data.
1042 Bioinformatics. 2014 Apr 1;30:2114–20.

1043 83. Gurevich A, Saveliev V, Vyahhi N, Tesler G. QUAST: quality assessment tool for genome
1044 assemblies. Bioinformatics. 2013 Apr 15;29(8):1072–5.

1045 84. Manni M, Berkeley MR, Seppey M, Simão FA, Zdobnov EM. BUSCO update: Novel and
1046 streamlined workflows along with broader and deeper phylogenetic coverage for scoring of
1047 eukaryotic, prokaryotic, and viral genomes. Mol Biol Evol. 2021 Oct 1;38(10):4647–54.

1048 85. Manni M, Berkeley MR, Seppey M, Zdobnov EM. BUSCO: Assessing Genomic Data Quality and
1049 Beyond. Curr Protoc. 2021;1(12):e323.

1050 86. Smit AFA, Hubley R, Green P. RepeatMasker Open-4.0. Available at:
1051 http://www.repeatmasker.org Accessed: November 30, 2017. 2013 2015;

1052 87. Palmer JM, Stajich J. Funannotate v1.8.1: Eukaryotic genome annotation. Zenodo; 2020.
1053 Available from: https://zenodo.org/record/4054262

1054 88. Brůna T, Hoff KJ, Lomsadze A, Stanke M, Borodovsky M. BRAKER2: automatic eukaryotic
1055 genome annotation with GeneMark-EP+ and AUGUSTUS supported by a protein database.
1056 NAR Genomics Bioinforma. 2021;3(1):lqaa108.

1057 89. Dobin A, Davis CA, Schlesinger F, Drenkow J, Zaleski C, Jha S, et al. STAR: ultrafast universal
1058 RNA-seq aligner. Bioinformatics. 2013;29(1):15–21.

1059 90. Jones P, Binns D, Chang HY, Fraser M, Li W, McAnulla C, et al. InterProScan 5: genome-scale
1060 protein function classification. Bioinformatics. 2014 Jan 5;30(9):1236–40.

1061 91. Krogh A, Larsson B, von Heijne G, Sonnhammer ELL. Predicting transmembrane protein
1062 topology with a hidden markov model: application to complete genomes. J Mol Biol. 2001 Jan
1063 19;305(3):567–80.

1064 92. Petersen TN, Brunak S, von Heijne G, Nielsen H. SignalP 4.0: discriminating signal peptides
1065 from transmembrane regions. Nat Methods. 2011 Oct;8(10):785–6.

1066 93. Käll L, Krogh A, Sonnhammer ELL. Advantages of combined transmembrane topology and
1067 signal peptide prediction—the Phobius web server. Nucleic Acids Res. 2007 Jul;35(Web Server
1068 issue):W429-432.

1069 94. Smit AFA, Hubley R. RepeatModeler Open-1.0.Available at: http://www.repeatmasker.org.
1070 Accessed: November 30, 2017. 2008 2015;

1071 95. Vogan AA, Ament-Velásquez SL, Bastiaans E, Wallerman O, Saupe SJ, Suh A, et al. The
1072 *Enterprise*, a massive transposon carrying *Spok* meiotic drive genes. Genome Res. 2021
1073 May;31(5):789–98.

1074 96. Gioti A, Mushegian AA, Strandberg R, Stajich JE, Johannesson H. Unidirectional evolutionary
1075 transitions in fungal mating systems and the role of transposable elements. Mol Biol Evol. 2012
1076 Oct 1;29(10):3215–26.

1077 97. Wicker T, Sabot F, Hua-Van A, Bennetzen JL, Capy P, Chalhoub B, et al. A unified classification
1078 system for eukaryotic transposable elements. Nat Rev Genet. 2007 Dec;8(12):973–82.

1079 98. Wyk S van, Harrison CH, Wingfield BD, Vos LD, Merwe NA van der, Steenkamp ET. The
1080 RIPper, a web-based tool for genome-wide quantification of Repeat-Induced Point (RIP)
1081 mutations. PeerJ. 2019 Aug 26;7:e7447.

1082 99. Debuchy R, Berteaux-Lecellier V, Silar P. Mating systems and sexual morphogenesis in
1083 Ascomycetes. In: Cellular and Molecular Biology of Filamentous Fungi [Internet]. John Wiley &
1084 Sons, Ltd; 2010. p. 499–535. Available from:
1085 https://onlinelibrary.wiley.com/doi/abs/10.1128/9781555816636.ch33

1086 100. Carver T, Harris SR, Berriman M, Parkhill J, McQuillan JA. Artemis: an integrated platform for
1087 visualization and analysis of high-throughput sequence-based experimental data.
1088 Bioinformatics. 2012 Feb 15;28(4):464–9.

1089 101. Sievers F, Wilm A, Dineen D, Gibson TJ, Karplus K, Li W, et al. Fast, scalable generation of
1090 high-quality protein multiple sequence alignments using Clustal Omega. Mol Syst Biol. 2011 Oct
1091 11;7:539.

1092 102. Waterhouse AM, Procter JB, Martin DMA, Clamp M, Barton GJ. Jalview Version 2--a multiple
1093 sequence alignment editor and analysis workbench. Bioinforma Oxf Engl. 2009 May
1094 1;25(9):1189–91.

1095 103. Emms DM, Kelly S. OrthoFinder: phylogenetic orthology inference for comparative genomics.
1096 Genome Biol. 2019 Nov 14;20(1):238.

1097 104. Abascal F, Zardoya R, Telford MJ. TranslatorX: multiple alignment of nucleotide sequences
1098 guided by amino acid translations. Nucleic Acids Res. 2010 Jul;38(Web Server issue):W7-13.

1099 105. Yang Z. PAML 4: phylogenetic analysis by maximum likelihood. Mol Biol Evol. 2007 Aug
1100 1;24(8):1586–91.

1101 106. Yang Z, Nielsen R. Estimating synonymous and nonsynonymous substitution rates under
1102 realistic evolutionary models. Mol Biol Evol. 2000 Jan;17(1):32–43.

1103 107. Marçais G, Delcher AL, Phillippy AM, Coston R, Salzberg SL, Zimin A. MUMmer4: A fast and
1104 versatile genome alignment system. PLOS Comput Biol. 2018 Jan 26;14(1):e1005944.

1105 108. Li H. Minimap2: pairwise alignment for nucleotide sequences. Bioinformatics. 2018 Sep
1106 15;34(18):3094–100.

1107 109. Li H, Handsaker B, Wysoker A, Fennell T, Ruan J, Homer N, et al. The Sequence
1108 Alignment/Map format and SAMtools. Bioinformatics. 2009 Aug 15;25(16):2078–9.

1109 110. Liu KH, Yeh YL, Shen WC. Fast preparation of fungal DNA for PCR screening. J Microbiol
1110 Methods. 2011 May 1;85(2):170–2.

1111 111. Rozen S, Skaletsky H. Primer3 on the WWW for general users and for biologist programmers.
1112 Methods Mol Biol Clifton NJ. 2000;132:365–86.

1113 112. Untergasser A, Cutcutache I, Koressaar T, Ye J, Faircloth BC, Remm M, et al. Primer3--new
1114 capabilities and interfaces. Nucleic Acids Res. 2012 Aug;40(15):e115.

1115

1116

1117

1118 **Supporting information captions**

1119

1120 **Supplementary note S1:** Frequency of second-division segregation of the mating-type
1121 locus under random segregation of the mating-type locus.

1122 **Supplementary Table S1:** Tests of differences in growth speed and dry weight between
1123 *Schizothecium tetrasporum MAT1-1 and MAT1-2* homokaryons and heterokaryons on
1124 different media.

1125 **Supplementary Table S2:** Genome assembly of the *Schizothecium tetrasporum*
1126 monokaryotic strains CBS815.71-sp3 and CBS815.71-sp6.

1127 **Supplementary Table S3:** List of 15 genes in the recombination suppression region around
1128 the mating-type locus in *Schizothecium tetraporum* predicted to encode proteins that are
1129 putative transcription factors or involved in signalling pathways.

1130 **Supplementary Table S4:** List of genes in the recombination suppression region around the
1131 mating-type locus in *Schizothecium tetraporum* having orthologues also located in the
1132 recombination suppression region around the mating-type locus in *Podospora anserina* and
1133 *Neurospora tetrasperma*.

1134 **Supplementary Table S5:** Quality of the raw reads produced and used in this study.

1135 **Supplementary Table S6:** PCR primers used in this study.

1136 **Supplementary Table S7:** PCR conditions used in this study.

1137 **Supplementary Figure S1:** Genome collinearity between the long read-based assembly
1138 and the Illumina-based assembly of *Schizothecium tetrasporum* CBS815.71-sp3 strain.

1139 **Supplementary Figure S2:** Transposable element annotation in different genomic regions
1140 of the *Schizothecium tetrasporum* CBS815.71 strain.

1141 **Supplementary Figure S3:** Amino-acid alignment of proteins containing a MATα_HMG
1142 domain.

1143 **Supplementary Figure S4:** Genome-wide distribution of synonymous divergence (dS) in
1144 the *Schizothecium tetrasporum* CBS815.71 strain. dS was computed per-gene between the
1145 CBS815.71-sp3 and CBS815.71-sp6 assemblies and plotted according to the CBS815.71-
1146 sp3 assembly gene position.

1147 **Supplementary Figure S5:** GC content variation and determination of centromeres the
1148 *Schizothecium tetrasporum* CBS815.71-sp3 assembly.

1149 **Supplementary Figure S6:** Delimitation of three evolutionary strata in the S*chizothecium*
1150 *tetrasporum* CBS815.71 strain.

1151 **Supplementary Figure S7:** Probability of recombination in centimorgans (cM) between
1152 markers and the mating-type locus in the heterokaryotic strain CBS815.71 after one round of
1153 experimental selfing measured in 107 of the offspring.

1154 **Supplementary figure S8:** Genome-wide collinearity based on single orthologous genes
1155 between *Neurospora crassa*, *Podospora anserina* and *Schizothecium tetrasporum* genomes.

1156

1157

1158

1159

1160 **FIGURES**

1161

1162 **Figure 1: Sexual reproductive structures and ascospores of *Schizothecium tetrasporum***
1163 **CBS815.71. A.** Perithecia on *Miscanthus* (1) and squashed perithecia showing the rosette of asci (2);
1164 bars = 200 µm. **B.** Enlargements of asci within the rosettes (1) and a five-spore ascus with three
1165 dikaryotic ascospores and two monokaryotic ascospores (2); bars= 20 µm. **C.** Other abnormal asci
1166 observed in CBS815.71: (1) a six-spore ascus with four monokaryotic ascospores (small) and two
1167 dikaryotic ones (large); (2) a five-spore ascus with three monokaryotic ascospores (the three small
1168 spores in the middle), one dikaryotic (the large ascospore at the bottom) and another, probably
1169 trikaryotic, ascospore (arrowhead showing the very large ascospore); bars= 20 µm.

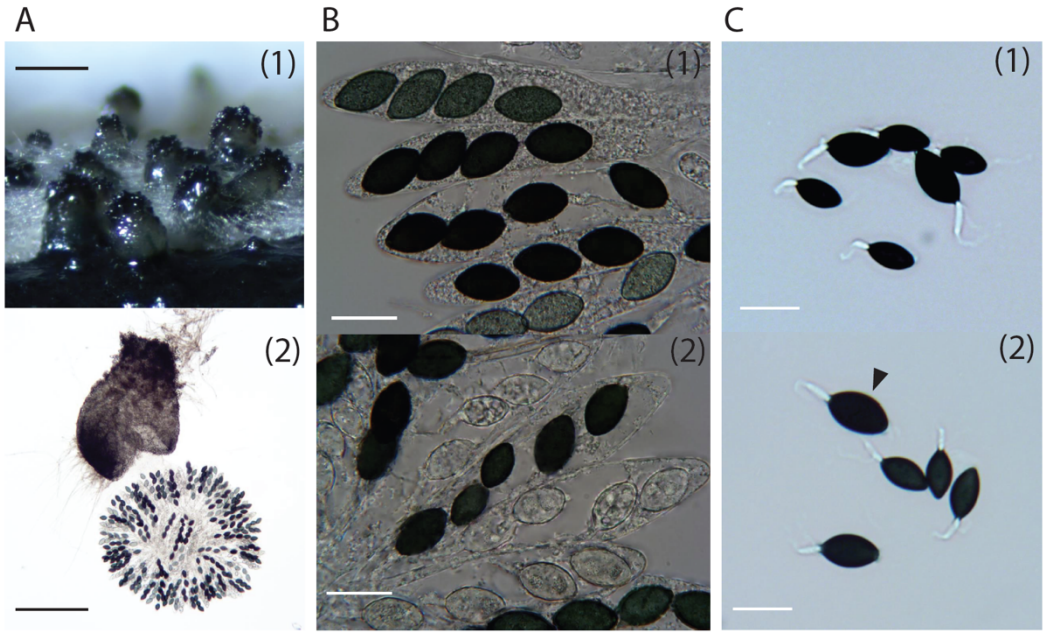

1170

1171

1172

1173

1174

1175 **Figure 2: Segregation of the mating-type locus during meiosis, ascus composition and**
1176 **hypothetical scenarios for the loss of one mating type in thalli of *Schizothecium tetrasporum***
1177 **A.** Theoretical composition of an ascus according to meiotic segregation pattern at the mating-type
1178 locus: if alleles at the mating-type locus (represented as a red or blue vertical bar) segregate during
1179 the first meiotic division (FDS, top), two *MAT-1-1* spores and two *MAT-1-2* spores are formed;
1180 conversely, if alleles at the mating-type locus segregate during the second meiotic division (SDS,
1181 bottom), four heterokaryotic spores carrying both mating types are formed. Only the chromosomes
1182 carrying the mating-type locus are represented, with their centromeres. The *MAT-1-1* and *MAT1-2*
1183 alleles at the mating-type locus are represented by red and blue vertical bars, respectively.
1184 Centromeres are represented by yellow circles at the diploid and meiosis I stages. Chromosomal
1185 arms are colored in red or blue according to the parental origin of the chromosomal fragment. **B.** Two
1186 hypothetical scenarios for the loss of one mating type despite SDS at the mating-type locus. SDS at
1187 the mating-type locus generates a spore carrying two nuclei of opposite mating types, but one nucleus
1188 may be lost during spore development (top) when half the nuclei gather in a region of the spore that
1189 subsequently undergoes apoptosis, or during mycelium growth (bottom).

1190

1191 **A**

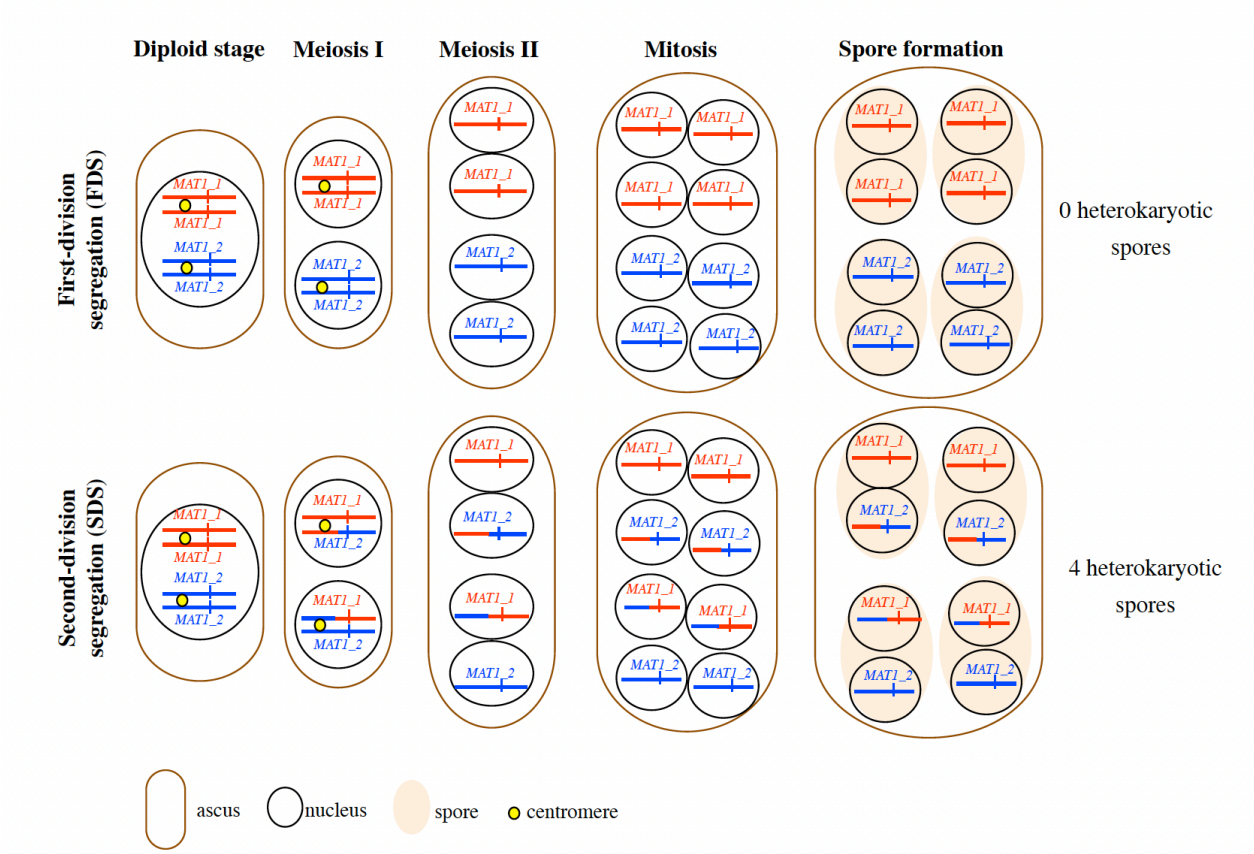

1192

1193

1194 **B**

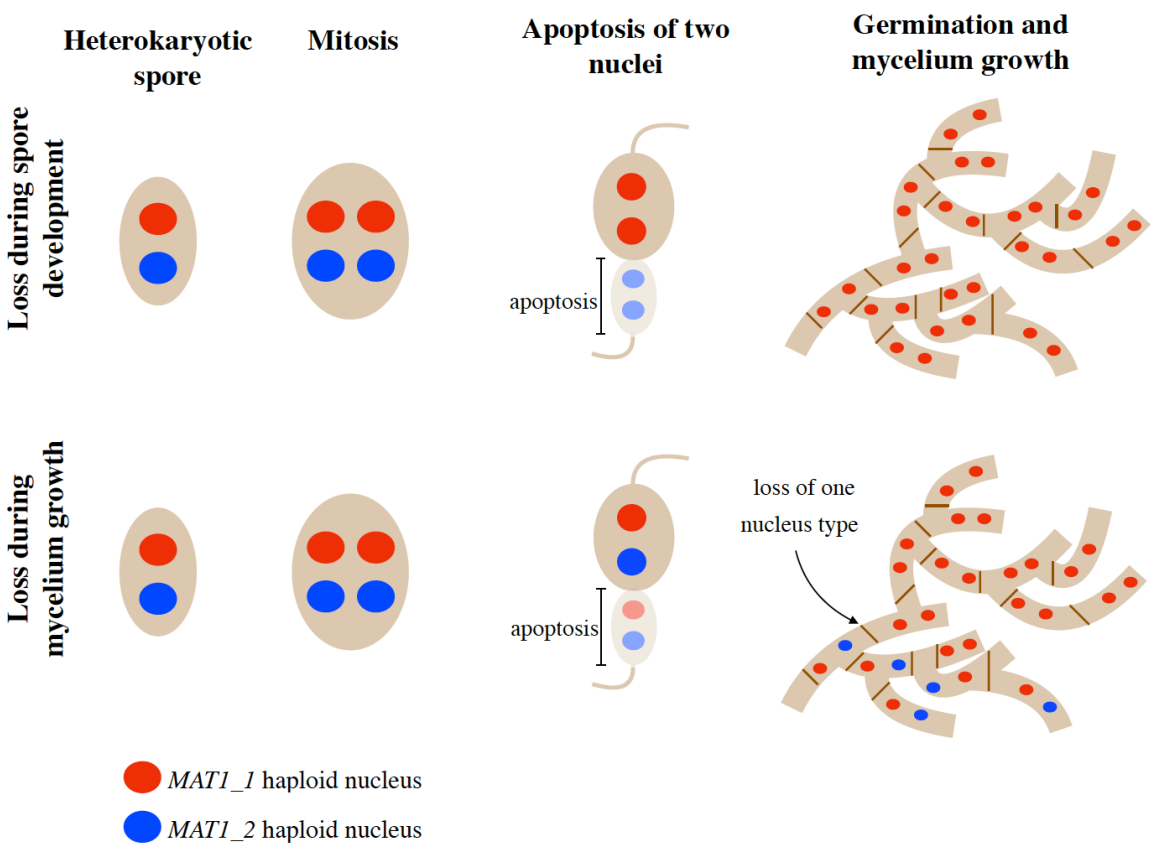

1195

1196

1197 **Figure 3: Genome features and annotation of the mating-type locus in the *Schizothecium***
1198 ***tetrasporum* CBS815.71 strain. A.** Ideograms representing the seven largest contigs of the
1199 CBS815.71-sp3 genome assembly. The mating-type locus is indicated with a green triangle, telomeric
1200 repeats with red boxes and putative centromeres with yellow circles. Gene density in 10 kb non-
1201 overlapping windows is represented by vertical bars on the contigs and the heatmap colors indicate
1202 low to high density. The non-recombining region around the mating-type locus is indicated by a black
1203 rectangle. **B.** Genome collinearity between opposite mating types of the *Schizothecium tetrasporum*
1204 CBS815.71 strain. Circular plot showing contigs from the CBS815.71-sp3 genome (green, right) and
1205 the CBS815.71-sp6 genome (purple, left). Only the largest contigs (>500 kb) were plotted. Blue links
1206 indicate the locations of orthologous genes (Mb). The mating-type locus is indicated with a green
1207 triangle. Putative centromeres and the non-recombining region around the mating-type locus identified
1208 on the CBS815.71-sp3 genome assembly are indicated by yellow circles and a black rectangle,
1209 respectively. **C.** Organization of the mating-type locus in CBS815.71-sp3 (top) and CBS815.71-sp6
1210 (bottom) assemblies viewed in Artemis v18.0.2 (100). The *APN2* and *SLA2* genes flanking the
1211 mating-type locus are indicated. The green boxes represent the nucleoide sequences differing
1212 between the two idiomorphs that were used to design markers for assessing mating type in the
1213 progeny. The *MAT1-1-1* pseudogene (*TαD1*) present in the CBS815.71-sp3 (*MAT1-2*) genome is
1214 boxed in red. The three forward and three reverse frames of the DNA sequence are presented;
1215 vertical bars indicate putative STOP codons.
1216

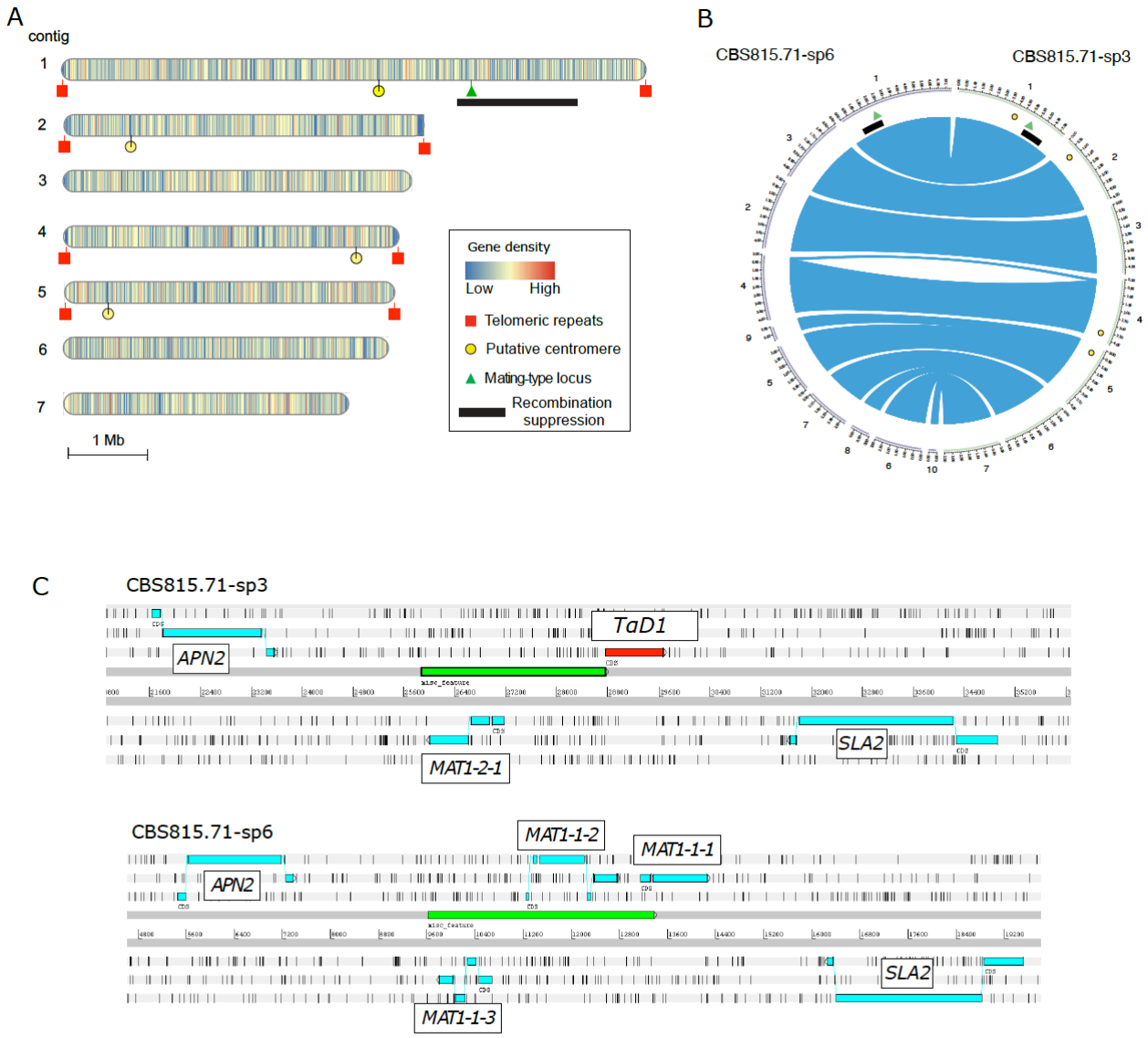
A
contig
1
2
3
4
5
6
7
1 Mb
Gene density
Low
High
Telomeric repeats
Putative centromere
Mating-type locus
Recombination suppression
B
CBS815.71-sp6
CBS815.71-sp3
C
CBS815.71-sp3
TaD1
APN2
MAT1-2-1
SLA2
CBS815.71-sp6
MAT1-1-2
MAT1-1-1
APN2
SLA2
MAT1-1-3

1217

1218

1219 **Figure 4: Synonymous divergence (d_S) along the mating-type chromosome in the**
1220 ***Schizothecium tetrasporum* CBS815.71 strain.** d_S was calculated per gene, between the orthologs
1221 common to the CBS815.71-sp3 and CBS815.71-sp6 assemblies and was plotted, according to the
1222 CBS815.71-sp3 assembly gene position (contig 1), along the *x*-axis. Evolutionary strata 1, 2, and 3
1223 are indicated by red, green and blue rectangles, respectively. The mating-type locus is indicated with
1224 a black dotted vertical line and a green triangle. The putative centromere is indicated with a yellow
1225 circle. The *P_NRR2* and *P_NRR5* markers, which displayed no recombination event with the mating-
1226 type locus, are indicated with gray diamonds.

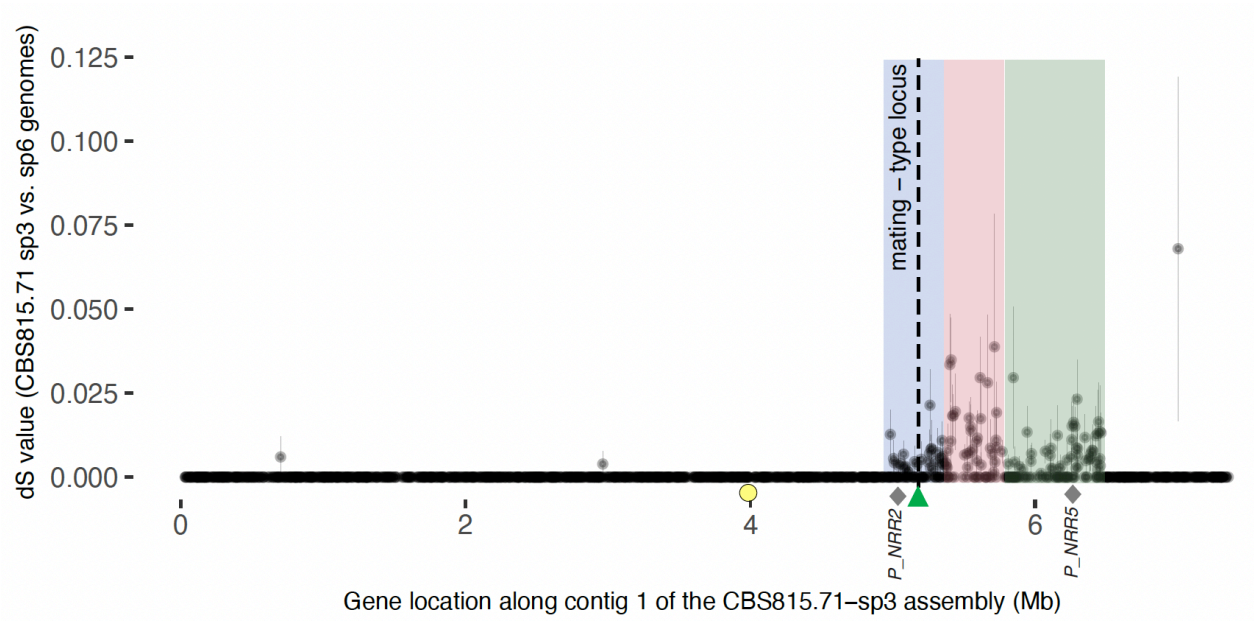

1227
1228
1229

1230 **Figure 5: Collinearity and shared gene content between the mating-type chromosomes of**
1231 ***Schizothecium tetrasporum, Podospora anserina* and *Neurospora tetrasperma*. A.** Collinearity
1232 between (i) *N. crassa* (left) and *P. anserina* (right); (ii) *P. anserina* (left) and *S. tetrasporum* (right);
1233 (iii) *N. crassa* (left) and *S. tetrasporum* (right). Collinearity is based on single-copy orthologous genes.
1234 Centromere is indicated with a yellow circle and the region of well-conserved gene order around the
1235 centromere is highlighted with a yellow rectangle. The mating-type locus location is shown with a
1236 green triangle and the non-recombining region around the mating-type locus in *P. anserina* (23) and
1237 *S. tetrasporum* with a black track. Along the recombining mating-type chromosome of *N. crassa* a
1238 black rectangle indicates the orthologous region that is non recombining in multiple *N. tetrasperma*
1239 lineages (26). Red, green and blue links highlight orthologous genes located in the evolutionary strata
1240 1, 2, and 3 of *S. tetrasporum,* respectively. Grey links indicate other orthologous genes. On panel (ii),
1241 the evolutionary strata identified previously in the *P. pseudocomata* CBS415.72 strain, that is closely
1242 related to the *P. anserina* S strain, are indicated by purple (for the oldest stratum) and dark green (for
1243 the youngest stratum) tracks (27), at left. B. Number of single-copy orthologous genes present in the
1244 non-recombining region of *S. tetrasporum* that are also in the non-recombining regions of *P. anserina*
1245 and/or *N. tetrasperma*, as indicated by the squares at the bottom (a filled square indicates the
1246 presence in the non-recombining region of the focal species).
1247

1248

A

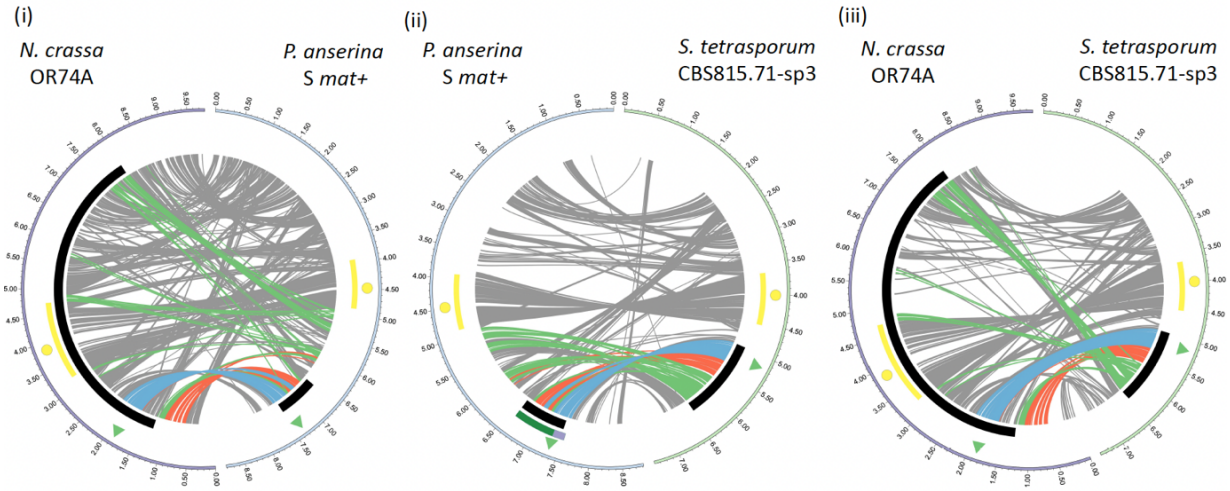

1249
1250

B

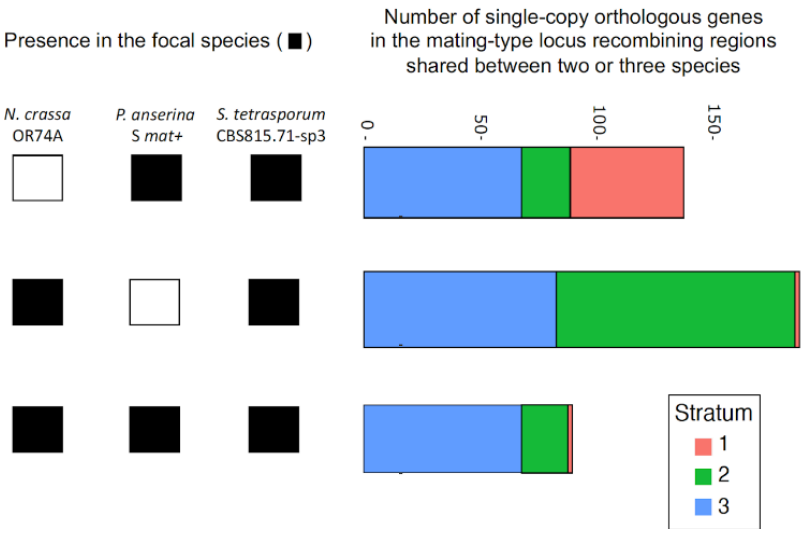

1251